

Technical University of Civil Engineering Bucarest

Leching effect on mechanical properties of cement paste and cement paste/aggregate composite

Scientific coordinators:

Prof. Dan-Paul Georgescu (UTCB)

Prof Moulay Saïd El Youssoufi (University of Montpellier)

Summary

| 1. | | | |
|----|-------------------------|------------------------------------|----------|
| 2. | | | |
| | 2.1. | Cement and aggregates | 3 |
| | 2.2. | Manufacture of local scale samples | 4 |
| | 2.3. | Accelerated leaching method | 6 |
| | 2.4. | Leaching kinetics | 9 |
| | 2.5. 2.5.1 2.5.2 | F | 12 |
| | 2.6. | Conclusion | 21 |
| 3. | Res | ults and discussion | 22 |
| | 3.1. | Leaching kinetics | 23 |
| | 3.2.1 3.2.2 3.2.3 | . Observation of cracking | 28 32 |
| 4. | Gen | eral conclusions | 38 |
| 5. | Bib | liography | 39 |

1. Introduction

Leaching is a phenomenon which appears following contact of concrete with a more acidic solution than the basic interstitial solution which occupies the porosity and which is in equilibrium with the cement paste. Thus, we are witnessing a decalcification which progresses gradually over time and generates the degradation of the mechanical properties of the material following the increase in porosity.

The degradation mechanism takes place through two main phenomena: diffusion and dissolution. The propagation of the leaching front and its kinetics are governed by the diffusion of the aggressive solution into the pore solution. Dissolution, especially of Calcium, occurs in the paste to ensure equilibrium with the acidified pore solution.

ITZ is a zone of the cement paste that forms around the aggregates with thicknesses of the order of a few tens of microns, having different physical properties compared to the bulk cement paste, such as higher porosity and different chemical species content. These features have major importance in the context of leaching because they make ITZ a more diffusive environment and more sensitive to chemical dissolution. There is therefore an objective risk of a local acceleration of the degradation kinetics, but also of a strong increase in porosity, with a significant effect on the adhesion of the paste to the aggregate.

In the context of studying the behavior of concrete at local scale, an experimental protocol was set up during Jebli's thesis (Jebli, 2016). This protocol consisted of creating a cement paste / aggregate bond and determining the mechanical properties. Jebli's thesis showed, in general, that the effect of leaching is more noticeable on the mechanical properties of the paste / aggregate bond than on those of the paste. It also showed the need to clarify some aspects related to ITZ. The main objective was to carry out more localized measurements of its degradation kinetics and mechanical behavior in the interfacial zone, in order to better define the role of ITZ in the degradation mechanism.

Therefore, in the present study, the two directions of study chosen relate to the degradation kinetics and the mechanical properties of concrete at the local scale. In order to be able to study these aspects, a simple geometry, but compatible, has been favored. This involves using cement paste and cement paste / aggregate composite samples with a square cross section. These samples are used to assess the progress of chemical degradation and the overall stress under mechanical loading. The progress of chemical degradation will be measured at the paste and ITZ level to determine their degradation kinetics. Regarding the mechanical behavior of samples at the local scale, it will be studied through mechanical tensile tests. The evolution of the mechanical properties of degraded samples at the local scale will be analyzed according to the progress of degradation.

2. Materials and methods

The need for a study at the scale of the paste / aggregate bond is dictated by a need to analyze the complex phenomenology which develops at the ITZ level and influences the mechanical behavior of concrete. Thus, in order to make such a study possible, an experimental protocol was developed to evaluate the effect of leaching on the mechanical properties of the paste / aggregate bond and on those of the paste.

In order to be able to evaluate the effect of leaching on the mechanical behavior of concrete on a local scale, it is necessary to evaluate the degradation kinetics and the effect of chemical degradation on the mechanical properties of the paste / aggregate bond. and paste. In this sense, samples with specific geometries are used.

On these samples, initially, the analysis of the degradation kinetics will be done in order to then make it possible to analyze the effect of degradation on the mechanical properties of the cement paste and the paste / aggregate composites.

Mechanical tests at the local level are intended to determine the mechanical properties of the paste / aggregate bond and of the paste in a sound and degraded state

2.1. Cement and aggregates

In industry, the choice of concrete formulation includes the dosage of constituents in order to meet the requirements of mechanical strength and durability. The formulation directly influences the quality of the cement paste / aggregate bond. Parameters such as cement type, admixtures, water / cement ratio and type of aggregate influence the ITZ composition, which in turn influences the physicochemical properties of the paste / aggregate bond.

With regard to the specific case of concretes subjected to leaching, they must guarantee sufficient mechanical resistance under aggressive environmental conditions thanks to suitable formulations. The w / c ratio directly influences the porosity of concrete in the hydrated state. The drop in the w / c ratio results in a decrease in porosity, which generates an increase in the strength and rigidity of the concrete, but it also influences the degradation kinetics. In a less porous medium, the diffusion coefficient is lower and, consequently, the degradation kinetics are slowed down. Moreover, the addition of pozzolans allows the consumption of portlandite to produce C-S-H. Thus, this addition contributes to the improvement of mechanical properties by increasing the amount of cohesive chemical species (C-S-H) and decreases the vulnerability to chemical attack following the dissolution of portlandite. The additions of the pozzolans are compatible with the drop in the w / c ratio to give rise to very high performance concretes which have compressive strengths much greater than 100 MPa. Apart from the w / c ratio and the addition of pozzolans, another important parameter in the choice of the formulation of such concrete is the type of aggregate. The choice of limestone aggregates is preferable to siliceous aggregates because the chemical reactions that occur between the limestone and the cement paste during hydration improve their adhesion and therefore, on a larger scale, the strength of the concrete.

In the case of the present study, the choice of materials aims to approximate the formulations of real concretes subjected to leaching and to give a perspective for the next studies. It is therefore a question of choosing a material with fairly high mechanical properties, but with a simple composition. Such a composition has the advantage of facilitating references to the literature and it can serve as a reference for future studies. This is why, on the one hand, we have chosen to avoid an overdose of water in order to acquire important mechanical properties and, on the other

hand, we have avoided the use of additives or secondary components like pozzolans. Therefore, the choice of materials used fell on a CEM I cement paste prepared with a w / c ratio of 0.4 and limestone aggregates.

2.2. Manufacture of local scale samples

In this paragraph, we present the experimental methodology used to manufacture, condition and store the specimens on a local scale. The samples fabricated for the microstructure analyzes as well as for the mechanical tensile and shear tests are cement paste parallelepipeds and cement paste / aggregate composites (Figure 1). The dimensions of the samples are 10x10x30 mm3. The composite sample is composed of an aggregate half (10x10x15 mm3) and a cement paste half (10x10x15 mm3) (Figure 1b).

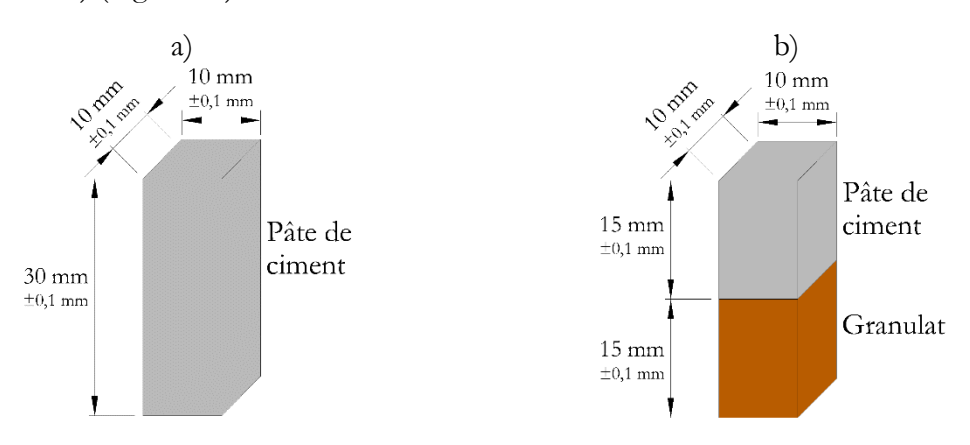


Figure 1 Cement paste a) and cement paste/aggregate samples b)

In order to ensure good representativeness of the samples, one requirement is to minimize the influence of the placement conditions on the measurement of the material properties. In this sense, one of the challenges is to ensure good dimensional repeatability and to minimize the impact of the manufacturing procedure on the properties of the material.

• Preparation of aggregates

In order to be able to manufacture the composite samples, aggregates with the desired shape were obtained from real rocks. The limestone aggregates were obtained from massive rocks from a quarry in Villeneuve les Maguelone (Hérault, France), before undergoing various cuts to achieve a parallelepipedal shape of 10x10x15mm3. The preliminary step is to cut from within the boulders plates with 17 mm thick parallel faces and 12 mm wide bars. Then, the aggregates were cut to the desired dimensions using a precision chainsaw of the Struers Secotom-15® type. This chainsaw has a fixed rotating grinding wheel and a sliding table which advances towards it with a speed of 0.5 mm / s.

In order to achieve the desired dimensions for the aggregates, a specific sample holder has been designed. The latter has the function of allowing cuts at a right angle and of adjusting the dimensions of the samples. The first step is to machine three faces of the aggregate so as to obtain a right trihedral angle between three faces of the sample. The second step consists in adjusting the dimensions of the aggregate in relation to the three reference faces. The aggregates were then measured and calibrated before sample preparation. Aggregates showing major defects or deformations were rejected. The end result is a parallelepipedal aggregate with perpendicular faces and a geometric tolerance of 0.1 mm (Figure 2).



Figure 2 Dimensions of aggregate (a) and set of 20 aggregates (b)

For the manufacture of the samples, flexible silicone molds were made. This type of mold has the advantage of being able to be produced quickly and in large quantities.

This material has been used by other experimenters (Öztekin et al., 2016) to make molds for concrete samples. These silicone molds have the advantage of allowing simple manufacturing that can be adapted to geometries that are not standardized.

Regarding the manufacture of the flexible latex molds used in the present study, they were made by pouring and polymerizing the liquid silicone around counter-molds with the desired dimensions (Figure 3). It has thus been possible to produce molds allowing the production of several samples in one casting and not requiring laborious preparation.

In addition to dimensional repeatability, these molds are waterproof, provide faces with good flatness and have non-adherent walls which also facilitate demoulding. Therefore, this type of latex mold was chosen for the manufacture of the samples.

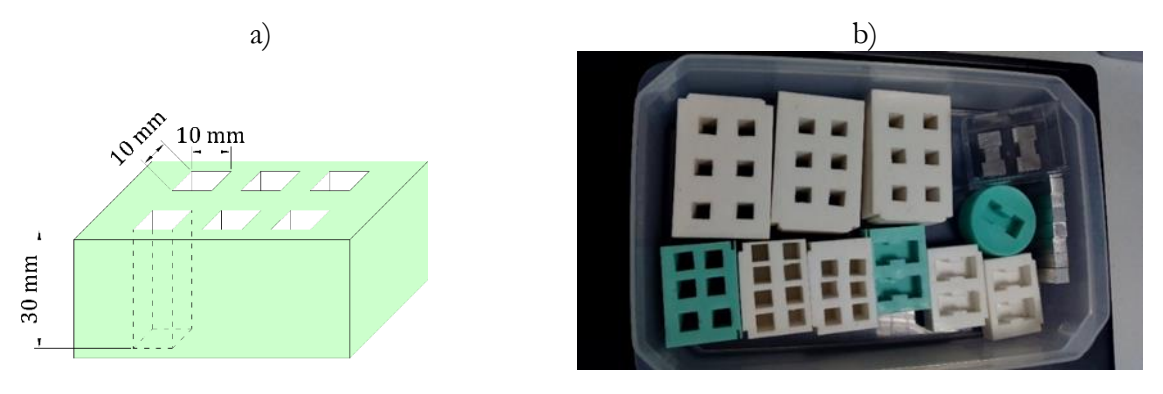


Figure 3 Latex molds dimensions (a) and example (b)

After manufacture, the test samples were kept in the mold for 24 hours in an environment at RH = 100%. Then, after demoulding, they were kept in a tank of water saturated with lime (Figure 4) for 40 days. This method of preservation allows optimal hydration of the material so that it achieves the required properties, and prevents any cracking due to desiccation.

After the forty-day hydration period, part of the samples was taken to test the properties of the sound material. The other part was leached to study properties of the degraded material.



Figure 4 Samples in lime saturated water solution

2.3. Accelerated leaching method

The leaching of concrete is a very long process compared to the times of laboratory studies. For example, it has been shown that for a certain type of macroscopic sample leached in water, a degraded thickness of 4 cm is reached after 300 years (Adenot, 1992). For experiments carried out in the laboratory, it is therefore necessary to use techniques to accelerate the rate of degradation. In this sense, several methods have been used in the literature, of which we quote:

- the application of an electric field;
- the use of solutions with an acidic pH relative to the pH of the concrete;
- the increase in temperature;
- the use of an ammonium nitrate solution;

The principle of applying an electric field across the test tube involves directing calcium ions from the anode to the cathode by applying an electrical potential difference across a test tube. Thus, very high concentrations of Calcium are obtained near the cathode while at the anode, Calcium is depleted. This method makes it possible to accelerate the rate of degradation by 50 to 500 times compared to the baseline scenario in pure water (Gerard et al., 1998; Le Bellégo et al., 2000; Saito et al., 1992). On the other hand, in this accelerated degradation scenario, several aspects differ from the baseline scenario. Indeed, the profile of the calcium concentration in the degraded zone is not similar to the case of degradation in water and the degradation rate is proportional to time, which does not take into account the diffusive phenomenon of the degradation.

Another solution for accelerating the rate of degradation is represented by the use of solutions with a relatively acidic pH compared to that of concrete (Revertegat et al., 1992) or by heating the degradation solution (Kamali et al. ., 2003). The advantage of these two types of methods is to obtain degradation kinetics proportional to the square root of time, similar to the base scenario (Revertegat et al., 1992). However, these methods allow the degradation rate to be accelerated up to 10 times compared to the baseline pure water scenario, which remains relatively long to reach the full degradation process in the laboratory within a reasonable time.

A final degradation method found in the literature consists of the use of a solution of ammonium nitrate as a chemically aggressive agent, in place of water. This method accelerates the rate of degradation due to the high solubility of hydrates in solution (Lea, 2012). First, upon diffusion, ammonium nitrate in a basic medium dissociates resulting in the reaction portlandite. The difference from the natural scenario is that the dissolution of portlandite begins at higher Calcium concentrations in the pore solution, therefore faster. Thus, the dissolution of portlandite is facilitated and the exchange of matter with the environment is accelerated due to the strong calcium concentration gradient between the pore solution and the external environment (Nguyen, 2005). The degradation in an ammonium nitrate solution exhibits kinetics proportional to the square root of time, specific to diffusive phenomena and therefore similar to the base scenario. This method achieves leach degradation rates 100 to 300 times greater than in pure water, hence a high rate. Another advantage of this method is the similar shape of the Calcium concentration profile in the degraded area with natural degradation (Figure 5) (Carde, 1996).

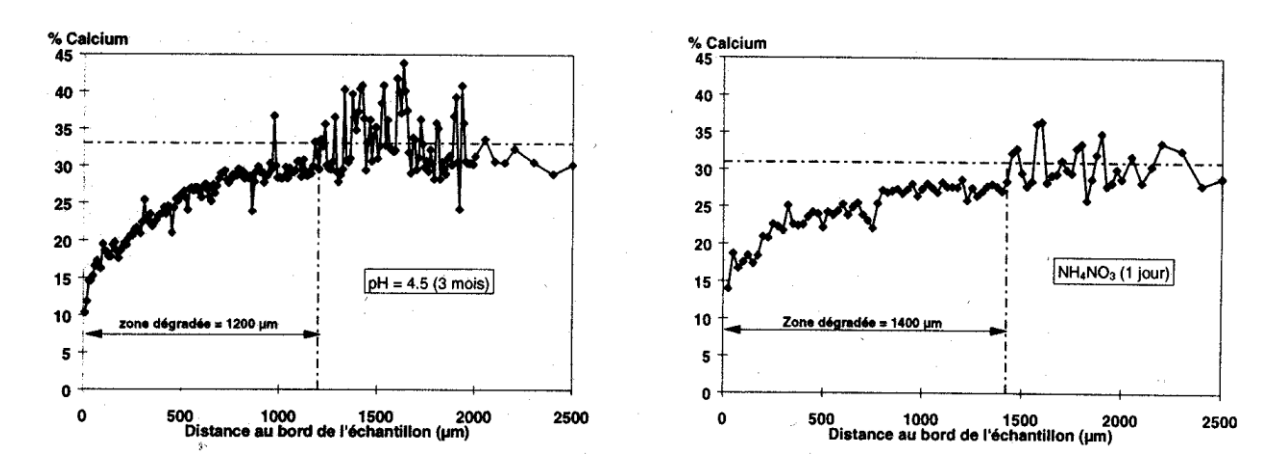


Figure 5 Calcium concentration profiles in degraded zone by demineralized water a) and ammonium nitrate b) (Carde, 1996)

Among the methods mentioned for accelerating degradation, the one chosen for the present study is the use of ammonium nitrate solution as an aggressive agent. This method was chosen thanks to its high rate of chemical degradation and to the similarity between the nature of the degradation process thus developed and the actual reference degradation scenario. Even if the degradation times are shorter locally, a significant acceleration would be appropriate thanks to the limitation of the analysis times and the possibility of carrying out several series of tests.

Regarding the concentration of the ammonium nitrate solution used to degrade the samples, it is similar to that used by other authors (Carde et al., 1996; Le Bellégo, 2001; Nguyen, 2005): 6 moles / liter. This corresponds to 480 grams of ammonium nitrate per 1 liter of water.

Besides the concentration, the amount of solution devoted to each sample influences the degradation process. It has been shown that as long as the pH of the aggressive solution remains below 9.25, its degradation power remains intact (Heukamp et al., 2002). The volume of ammonium nitrate solution devoted to each sample was set to meet this condition and avoid renewal. This volume, denoted V_s , was calculated according to a relationship that exists in the literature (Le Bellégo, 2001):

$$V_{\rm s} = 0.048C\gamma V_{\rm d} \tag{2.1}$$

where, C (gram / liter) is the cement content of the material subjected to degradation, γ (%) is the percentage of Calcium oxide in the anhydrous cement and V_d (liter) is the volume of the material subjected to degradation.

Following the choice of the characteristics of the aggressive solution, the establishment of the degradation was completed by the choice of its geometric configuration and by the way of distributing the samples.

Concerning the geometrical configuration of the degradation, it was carried out by putting in contact 2 opposite longitudinal faces with the aggressive solution. The other sides were protected by applying waterproof tape before dipping the samples into the ammonium nitrate solution (Figure 6). The samples were thus subjected to a unidirectional degradation which propagates perpendicularly to the faces attacked by the aggressive solution.

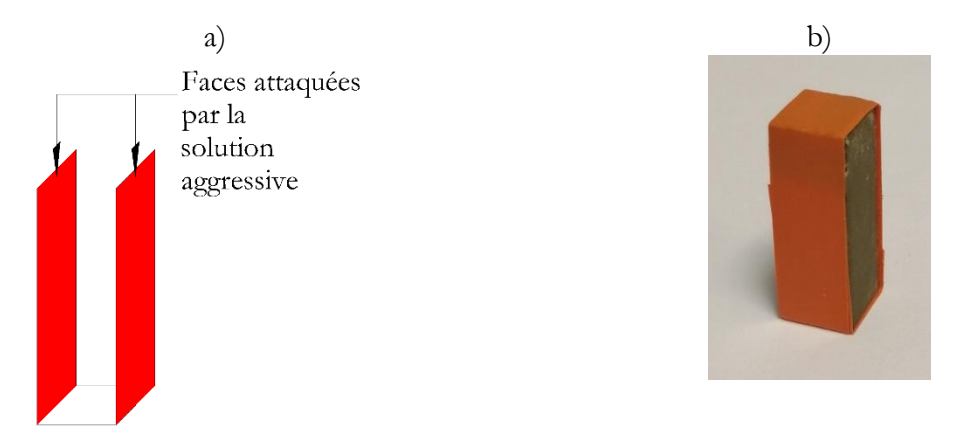


Figure 6 Leaching kinetics configuration illustration and (a) example (b)

This gives rise, in cross section, to the appearance of two degraded areas on both sides of the sound area in the middle (Figure 7). The choice of this unidirectional degradation configuration is dictated by a need to ensure uniformity of degradation fronts across thickness. This is preferred in order to facilitate interpretation of the effect of chemical degradation on the mechanical properties of samples.

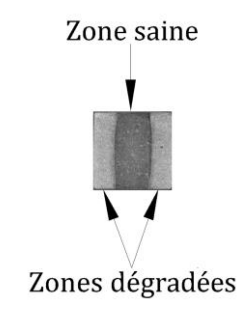


Figure 7 Cross section of degraded sample

Then, in order to finalize the establishment of the chemical degradation, the samples were degraded individually at constant ambient temperature. In fact, each sample is degraded in its container, with the same volume of aggressive solution, sufficient to avoid renewal (Figure 8). This method of individual degradation ensures uniform conditioning of all samples, in the absence of mechanical agitation. This mechanical agitation is a method that serves to homogenize a solution in which all the samples are kept together. (Le Bellégo, 2001; Nguyen, 2005).

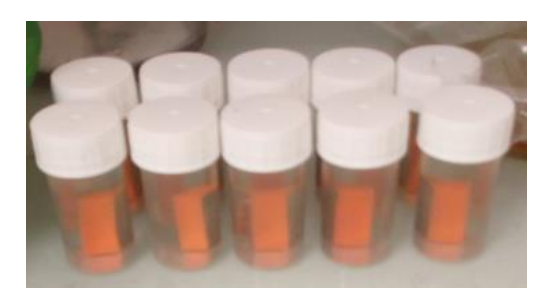


Figure 8 Individual leaching method

The samples thus degraded were subjected to leaching for several degradation times: 0.75; 2; 4; 8; and 12 days. At each time step, the samples intended for mechanical tests were taken and stored in water until the test at least one day.

2.4. Leaching kinetics

Knowledge of the degradation kinetics is necessary in order to determine the state of degradation, but also to subsequently interpret the effect of leaching on the mechanical properties of the paste and of the paste / aggregate bond.

In order to determine the degradation kinetics, several methods have been used in the literature. These methods are mainly intended to locate the position of the degradation front from which the degraded thickness is determined for different degradation times. In some cases, they can provide additional information on the nature of the degradation. The most widely used methods in the literature for measuring degraded thickness are color indicators, EDS measurements and optical microscope observations (Figure 9).

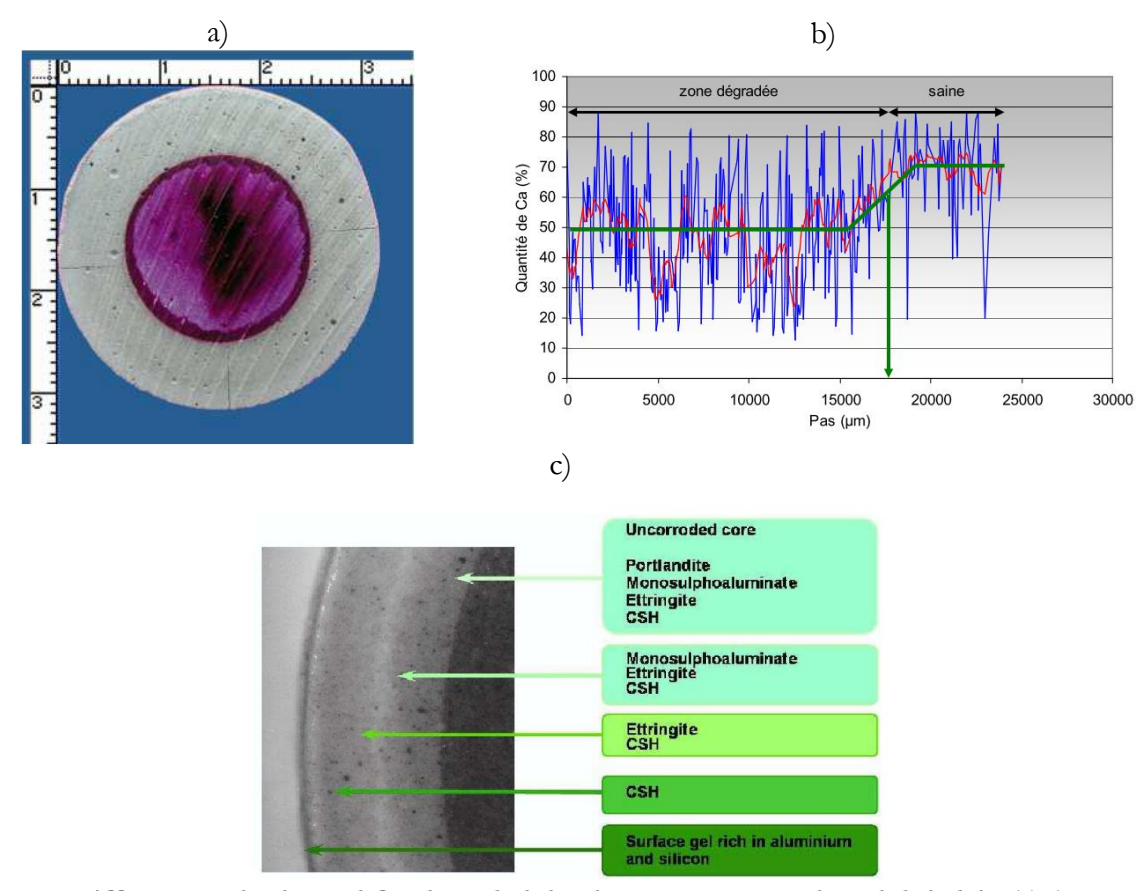


Figure 9 Different methods used for degraded depth measurement. phenolphthalein (a) (Nguyen, 2005); Measurement through Calcium concentration profiles(b) (Camps, 2008); Optical microscope measurement (c) (Adenot and Faucon, 1996)

The most widely used color indicator is phenolphthalein, which applied to a cross section, generating a color change that allows the delineation of the sound area and the degraded area. In the initial state it is colorless but it turns pink when in contact with solutions with a pH above 11. Therefore, by applying phenolphthalein on a cross section of a concrete sample, the sounf area turns pink and the degraded area keeps its natural color (Figure 9a).

However, considering that the pH of the interstitial solution in the sound zone is close to 13, therefore greater than 11 (value associated with the color change), the thickness of the colorless zone is not equal to the thickness of the degraded area. It is still possible for concretes based on CEM I (pure portland cement) to calculate the exact value of the degraded thickness using the formula (Le Bellégo, 2001):

$$e_d = 1,17 * e_{ph} (2.2)$$

where e_d the actual degraded thickness and e_{ph} represents the degraded thickness measured with phenolphthalein

The advantage of this method of measuring the thickness degraded by phenolphthalein is the simplicity and speed which makes it possible to analyze a large number of samples at the same time. The drawbacks are linked to its limitations: it does not provide information on the local state of degradation and does not give direct access to the degraded thickness.

Another method of measuring degraded thickness is represented by chemical analysis EDS (Energy Dispersive X-ray Spectroscopy) which also makes it possible to locate the degradation front on chemical concentration profiles. On a linear concentration profile produced in the direction of degradation, the position of the degradation front corresponds to the point where the calcium concentration reaches the mean value of the non-degraded zone (Camps, 2008; Carde et al., 1996; Le Bellégo, 2001). Beyond the location of the degradation front, this method also provides access to the profile of elemental concentrations in the degraded area. Thus, according to the calcium concentration profile, two degradation sub-zones can be distinguished (Figure 9 b).

The advantages of this method lie in the possibility of direct chemical analysis which allows the localization of the two degradation fronts and provides information on the nature of the chemical degradation. In fact, the main degradation front is the dissolution front of portlandite while the intermediate front is that of C-S-H decalcification. The disadvantages of the method lie in the difficulty of sample preparation. The specific polishing required requires long and laborious handling.

A final method of determining the kinetics found in the literature and considered relevant for the present study is represented by optical observation. This kind of observation allows the localization of degradation fronts according to the position of the color change in the degraded zone. Several authors (Adenot and Buil, 1992; Kamali et al., 2003) have used optical observations coupled with chemical analyzes to locate, as appropriate, the main degradation front and / or the intermediate front (Figure 9).

The advantage of this method is represented by a relatively simple implementation, which gives good representativeness, despite certain limitations. In reality, this method allows the measurement of degraded thickness, but does not provide direct access to chemical concentrations. Therefore, for the validation of the degraded thickness measured by optical observations, chemical analyzes may be necessary. Nevertheless, the comparison of the results obtained by optical observations and by chemical analyzes showed a good agreement, thus validating the method of measurement by optical observations.

Therefore, taking into account the advantages and disadvantages of each of the methods presented, it was decided to resort to optical observations for the measurement of the degraded thicknesses. The tool used, an optical scanner, allows the measurement of gray levels with resolutions up to 2µm. The sufficient contrast between the gray level of the sound zone and that of the degraded zone made possible their delimitation and therefore the measurement of the degraded thickness for several degradation durations.

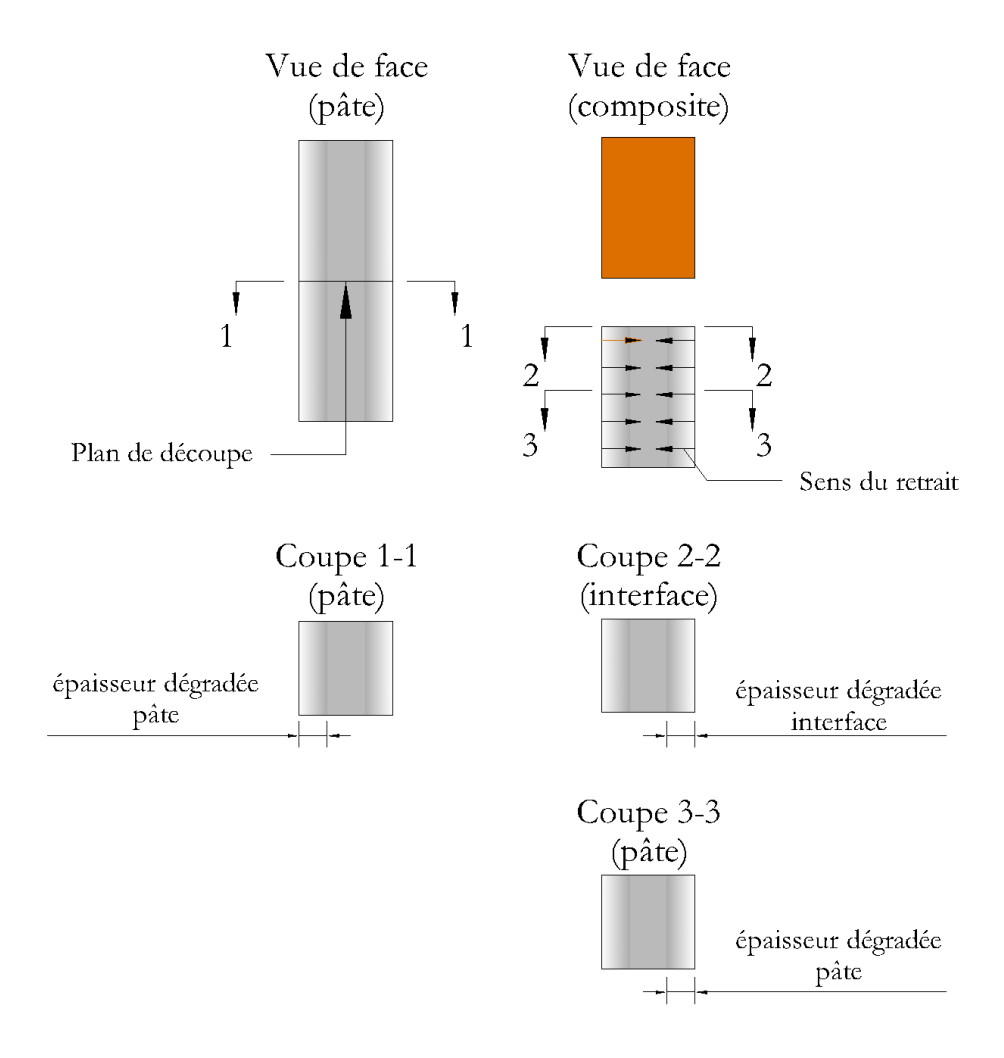
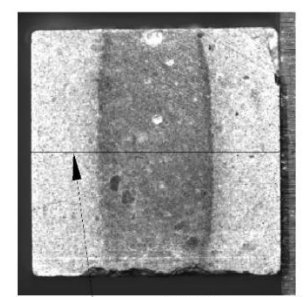


Figure 10 Cross sections of cement paste and composites samples for degraded depth measurement

The degraded thickness measurement was carried out on parallelepiped samples of cement paste and paste / aggregate composites, cast vertically, for each degradation period, in order to determine the degradation kinetics. The degradation kinetics analysis was performed on cross sections of degraded samples (paste and composites) (Figure 10).

Measurements of the degraded thicknesses of the composites were made at the core of the cement paste and at the interface. The measurements at the interface were possible following the decohesion of the composites, favored by the removal of desiccation. By storing the composite samples in an atmosphere with an RH of between 60% and 70%, a loss of adhesion occurs between the paste and the aggregate following the desiccation withdrawal of the paste (Monteiro and Mehta, 1985). Thus the two parts paste and aggregate can be detached.

The measurement of the degraded thickness was carried out by observing the gray levels on the median of the cross sections (Figure 11). The dynamics of the digitization of the images generated a scale of gray levels between 0 and 255. Consequently, the evolution of the gray level in the analyzed zone allowed the localization of the degradation front following the differences which exist between the values. gray levels encountered in the sounf zone and those encountered in the degraded zone. For reasons of measurement noise, the point gray levels were obtained by averaging the values of the pixels located in a zone of 10 pixels around the point considered.



Médiane de la section (ligne de calcul du niveaux de gris)

Figure 11 Region of interest for degraded depth measurement

2.5. Mechanical tests at local scale

The mechanical properties of sound concrete or concrete degraded by leaching are limited by the characteristics of the bonds which form between matrix (paste) and skeleton (aggregates). The specific behavior of the paste / aggregate bond is linked to peculiarities of the ITZ microstructure which differentiates it from the core of the cement paste.

It is in this context, that in the present study, the mechanical behavior of concrete at the local scale of the paste / aggregate bond is studied on composite paste / aggregate samples, taking paste samples as a reference. On these two types of samples, the mechanical properties are observed using mechanical tensile tests.

In the processing of the results of these mechanical tests, a fundamental component is represented by the measurement of displacements and deformations, carried out by Digital Image Correlation (CIN). This technique is especially useful for accessing the stiffness moduli of the material analyzed. Apart from this, the coupling between the CIN strain measurements and the observation of the mechanical loading during the test allows the optimization of the test devices.

2.5.1. General presentation of the testing device

The general test set-up assumes the application of a mechanical load and detection of the response of cement paste and paste / aggregate composite samples. This device is therefore composed of a test machine and a video camera (Figure 12). The testing machine is used to apply and measure the force supported by the sample it is applying. The video camera, on the other hand, is accompanied by a light source, and is used to record the movement of samples during loading to determine, in the observation focal plane of the camera, displacements and deformations.



Figure 12 Testing set-up

As for the testing machine, it is an MTS tension / compression press consisting of a fixed table and a movable cross member with only one degree of freedom - the vertical translation. In order to carry out the planned tests, the test frame is connected between the fixed table and the mobile cross member, while the desired loading is carried out following the translation of the mobile cross member. During the test, the machine allows the measurement of the force applied thanks to an associated sensor, but also the measurement of the displacement of the mobile cross member. For each type of test carried out, the loading was controlled while moving, with a constant speed of $10 \, \mu m$ / second imposed on the cross member.

In processing the test results, the value of the applied force measured by the machine is considered reliable for the load supported by the sample, because the energy losses at the test frame are negligible. In contrast, the measurement of sleeper displacement is not representative for the sample, as it includes the displacements of all components of the test frame. It is for this reason, in fact, that the use of an alternative method is necessary for the measurement of the deformations of the samples.

The method chosen for the measurement of sample deformations is digital image correlation (CIN), which has the advantage of allowing observation of the sample as a whole during stress. CIN is a technique developed to carry out measurements of displacement and strain fields, from successive images of the body observed on a filmed surface. Using this technique, points defined on a reference image are located on the images distorted during stress using iterative algorithms to determine point displacements. Thus is obtained the field of displacement, while the fields of deformations are obtained by the derivation of the field of displacement. By convention, the sign of the deformations is considered positive for expansion and negative for contraction.

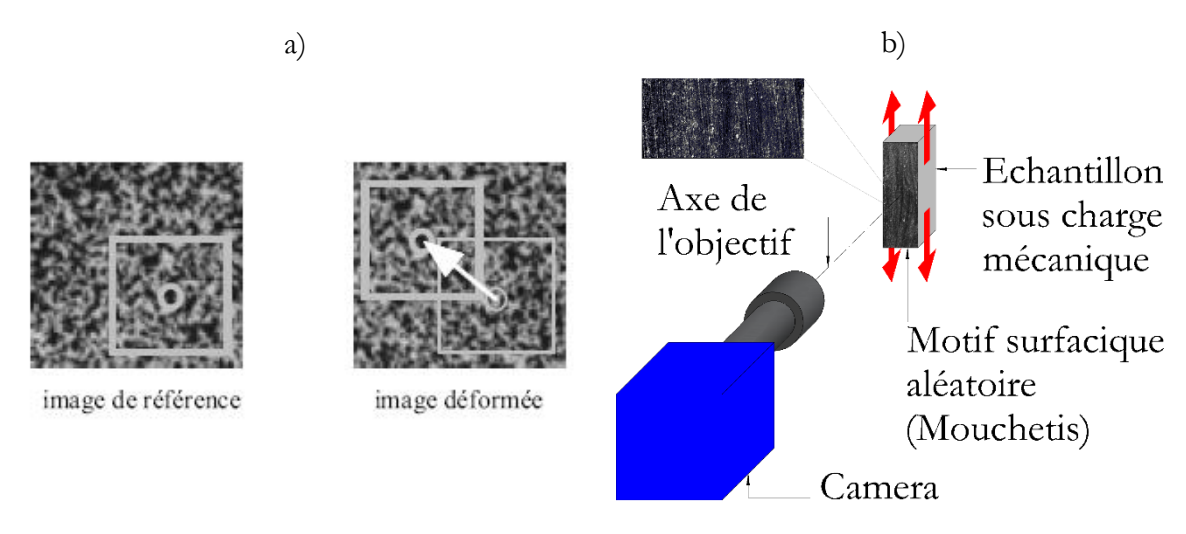


Figure 13Digital image correlation principle. Localisation of correlation zone within research zone (Hild, 2004) (a); Digital image correlation observation on a randomly patterned face (b)

To allow the measurement of point movements, the points sought are defined in the reference image by the gray levels of the pixels located in a correlation zone centered around the point concerned. Then, the position of this correlation zone is localized on the distorted images within a larger search zone, following successive iterations (Figure 13a). Under these conditions, in order to be able to define and then distinguish the correlation zones in the successive images, it is necessary to have a random distribution of the points both in terms of their shape and their gray level, on the analyzed surface. In the absence of such a naturally heterogeneous surface, this

requirement is often met following the application of a speckle on the surface observed by CIN. For the present study, this kind of speckle was obtained by applying light spots on a dark background (Figure 13b). Following the application of the speckle, the displacement and deformation was measured using the Trait Cine NRJ software developed at LMGC which operates according to the principles mentioned by Wattrisse et al. (Wattrisse et al., 2001).

Regarding how to use the CIN, two possibilities stand out depending on the information sought: either to promote the rate of recording, or to promote the resolution of the measured fields.

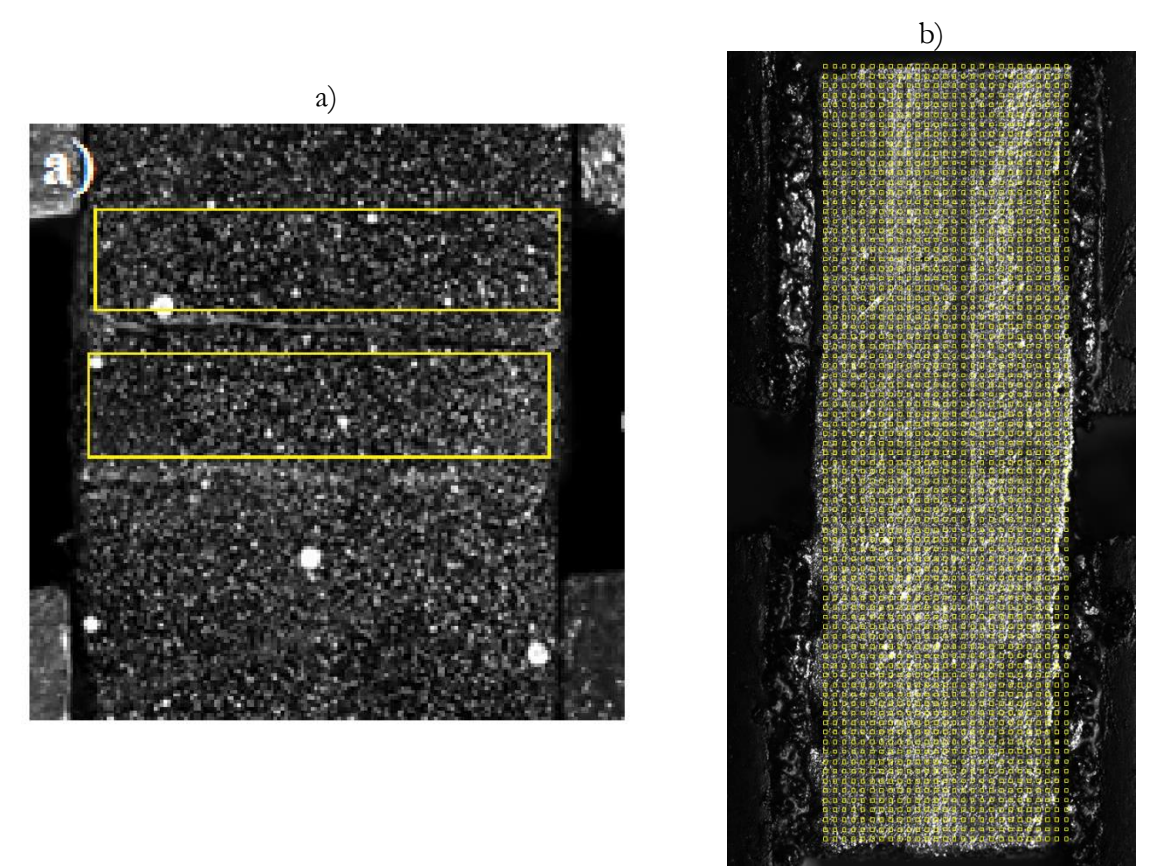


Figure 14 Region of interest for displacement and strain fields by high speed camera (Jebli, 2016)

(a) and by high resolution camera (b)

The first possibility, that of promoting the recording rate, is represented by the use of a high speed camera to record the movement of the sample during the solicitation. The advantage of this possibility is to be able to observe the sample throughout the test, including during rupture, thanks to recording frequencies which can vary between 10,000 and 40,000 images per second. This method was used by Jebli (Jebli, 2016) for the same types of mechanical tests carried out in the present study, direct tensile and shear. Using this method, the deformations associated with the forces measured by the machine were calculated by a procedure similar to an extensometer-type measurement, between two surface elements located in the area of interest (Figure 14 a). The ruptures observed using this method have been shown to be fragile, with sudden dissipation of energy.

Therefore, the use of a high speed camera was found to be useful at first to observe sample breakage. In the present study, the same kind of rupture was observed on the samples analyzed. Therefore, considering the behavior at break of these known samples, it was decided to widen the observation fields of the samples, by increasing the surface resolution of the calculated fields.

This was possible following the use of a high resolution camera, with a maximum resolution of 16 MPx, which corresponds to $7.7x7.7~\mu m^2$ / px, but whose recording rate was much lower, 4 -5 images / second. Using this method, displacement and strain fields could be calculated with a better definition on the surface of the samples observed, by increasing the number of point measurements carried out (Figure 15b).

However, due to the high resolution of the images, the use of this type of camera required more rigor in the realization of the speckle. A speckle which ensures a dispersed and varied arrangement of the gray levels on the observed surface results in a reduction in the size of the spots, but which also covers a wide range of gray levels. Therefore, the speckling technique has been adapted to these requirements by reducing the size of the white paint spots applied and / or by applying shiny flakes.

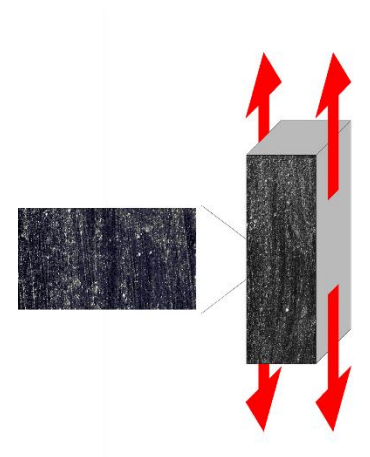


Figure 15 Example of ramdom pattern applied on sample's surface subjected to tensile test

In summary, a test device was implemented to observe the mechanical behavior of cement paste and paste / aggregate composites samples for different types of tests. This general device allows the measurement of the force exerted on samples subjected to mechanical stresses, as well as the measurement of their displacement and strain fields. Different types of tests can be obtained by adapting the frame connected to the testing machine, through which the envisaged mechanical stress is achieved.

The different types of mechanical tests carried out on cementitious materials are used to characterize their behavior from the elastic range to failure. Although this type of material is most often used for its compressive strength, the general mechanical behavior is influenced by the way in which the material resists local failure. These local ruptures appear and propagate in different modes of cracking, following tensile stresses (mode I), shearing (mode II) and torsion (mode III).

Therefore, the types of tests used in this study tend to reproduce this type of stress, in order to explore the ability of materials to withstand them. In the treatment of these tests, it was chosen to focus on the behavior of materials up to the peak load, favored by the use of a high resolution camera. It should be noted that a study of the propagation of cracking is necessary, but this requires more complex instrumentation and may be addressed in subsequent studies.

2.5.2. Testing device

The observation of cementitious materials under load has resulted in the deduction of failure criteria which reflect their ability to withstand mechanical stresses. The failure criteria applicable to concrete, such as Drucker-Prager or Mohr-Coulomb, indicate that these materials are more vulnerable to tensile stresses. Their reduced tensile strength is limited by the presence of pasteaggregate bonds, which are weakened by the existence of ITZs and which promote rupture initiation.

As a result, it was chosen to primarily promote the study of the mechanical behavior of the paste / aggregate bond and that of the paste on this type of stress, which is the most aggressive for the material. Therefore, the type of test discussed was that of direct traction. This type of mechanical test was performed on paste samples, as well as on composites cast vertically and horizontally.

Using the general test device presented in paragraph 2.5.1, the tensile tests were carried out according to a loading scheme implemented by Jebli (Jebli, 2016). According to this loading scheme, the application of the load to the specimens is done by means of metal plates glued to the side faces of the specimens (Figure 16).

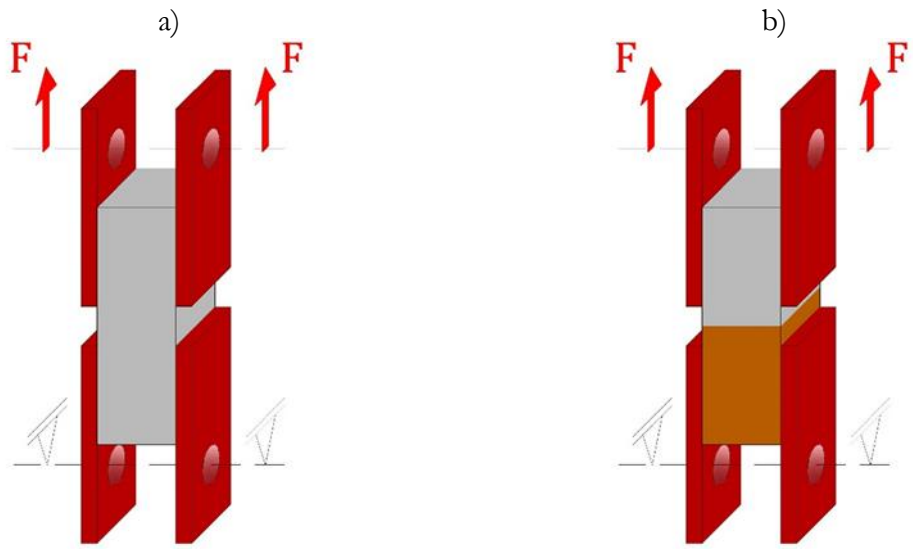


Figure 16 Representation of tensile test loading system for cement paste a) and composite sample b)

The calculation of the displacement and strain fields was carried out on the face of the sample which was filmed during the strain (Figure 17). The calculation of the mean strains was carried out to construct the stress / strain curves in the middle zone of the sample (Figure 17) in order to avoid the particular boundary conditions at the plate levels. The mesh step chosen for the displacement calculation is 50 pixels - 350 μm .

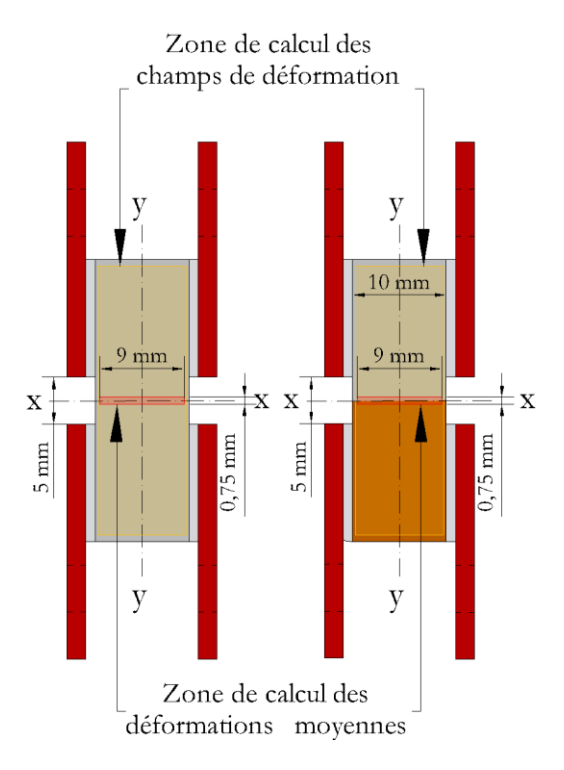


Figure 17 Front view of region of interest for digital image correlation of samples

The displacement fields were studied in particular to detect the appearance of cracking, because significant cracking was noted on the degraded samples. On the displacement fields, the cracks are visible on the image as areas of discontinuity (Figure 18).

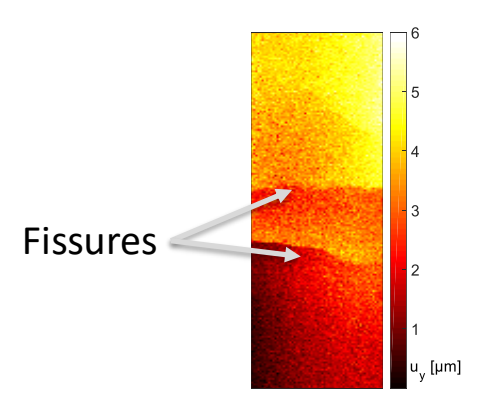


Figure 18 Cracking of a cement paste sample

2.5.2.1. Complementary accessories

Tensile tests on concrete are often marred by a strong dispersion of results, especially in terms of stress at break. In general, the large dispersion of the forces at failure is partially linked to an eccentricity of the loading inherent in the conditions of setting up the test (Zhou, 1988).

Therefore, a significant amount of non-representative tests for the measurement of actual breaking stresses should be excluded in the analysis of the results (Lhonneur et al., 2019). The strategy adopted to decrease the dispersion of the results was to standardize the imposed boundary conditions of loading, by limiting both the geometric defects of bonding and reducing their influence on the uniformity of the loading.

The solution adopted to limit geometric defects is represented by the use of bonding arrangements intended to ensure satisfactory positioning of the plates. Two types of assembly were tested: on the one hand, an assembly based on a drilled plate and on the other hand, a square and an assembly formed by two rigid guided half-boxes.

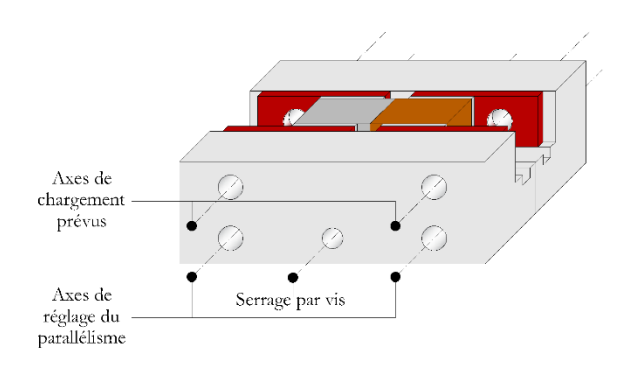


Figure 19 Device used for gluing of loading plates

The adhesive assembly used consists of two rigid and guided half-boxes (Figure 19b). The two axes of adjustment of the parallelism located in the lower part of the assembly were intended to allow only the relative translation of the half-boxes. The four mounting plates were then positioned inside the frame with the two jaws apart. The whole thing was then tightened through the screw at the bottom. This set-up allowed the parallelism of the plates and the load application axes to be satisfactorily adjusted and was selected for use in preparing samples for testing.

The geometric precision of the assembly is expressed by the maximum parallelism error at the level of the loading axes. This precision has been obtained by minimizing the play between the positioning pins and their holes. It is expressed by the maximum distance between an imaginary line which connects the centers of the holes of two plates located face to face and a horizontal line which passes through the center of the first axis taken as a reference. The value thus obtained is equal to 0.1 mm.

Once the geometric defects had been reduced to a satisfactory value, the loading device was examined. The initial loading device consisted of two U-shaped pieces rigidly linked to the testing machine and each connected, via a pivot, to the sample loading plates. The problem with this loading device was that the axis of the loading pivot did not coincide with the axes of the mounting plates due to geometric imperfections in the bonding. The system was then hyperstatic and required the release of at least one degree of freedom to load all the plates evenly.

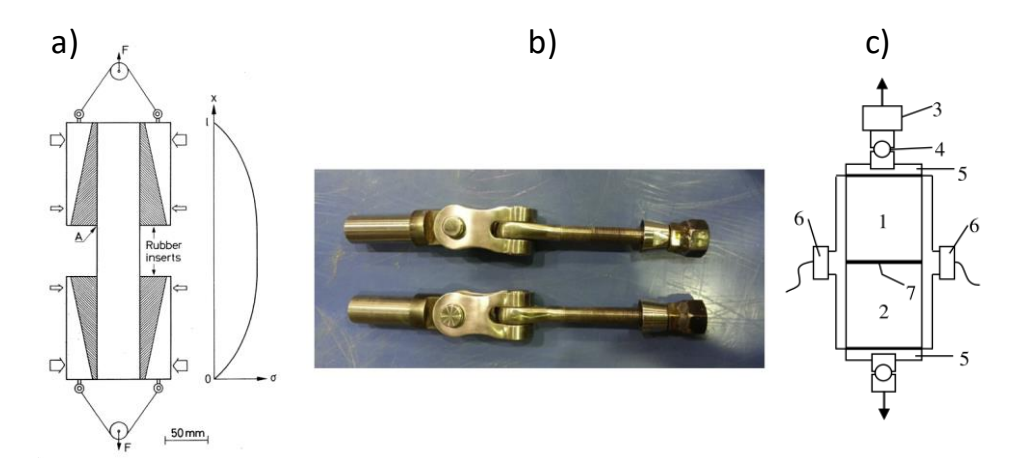


Figure 20 Different devices used to solve accidentally eccentricity problem (Alhussainy et al., 2016; Dong et al., 2016; Petersson, 1981)

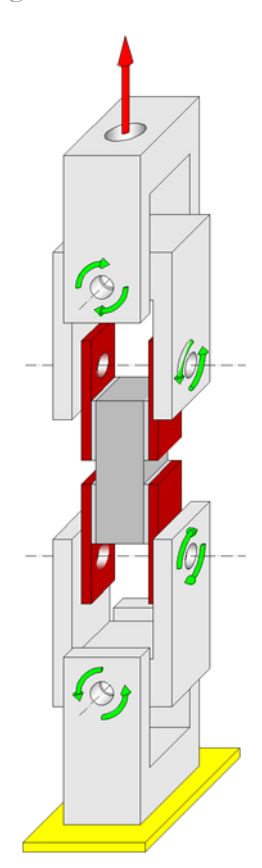


Figure 21 Tensile test loading device

To overcome this defect, it was necessary to add a mechanism to allow centered loading. Indeed, this load centering problem is known and has been mentioned in the literature as a major difficulty in carrying out tensile tests on concrete (Mier and Vliet, 2002). Several solutions, three of which we will briefly mention, have therefore been proposed. A rig with two pulleys and cables tied to the fixing plates was used by Petersson (Petersson, 1981) (Figure 20a). Alhussainy (Alhussainy et al., 2016) used two universal joints which free the rotations (Figure 20 b) while spherical ball joints were used by (Dong et al., 2016; Ferro, 1994) (Figure 20 c)

The loading device used is bi-articulated in the upper and lower parts (Figure 21). This was achieved by adding two U-pieces drilled during the initial assembly, linked to the fixed U-pieces via two pivots. Thus, at both ends of the sample, the rotations are released around two orthogonal axes perpendicular to the loading direction.

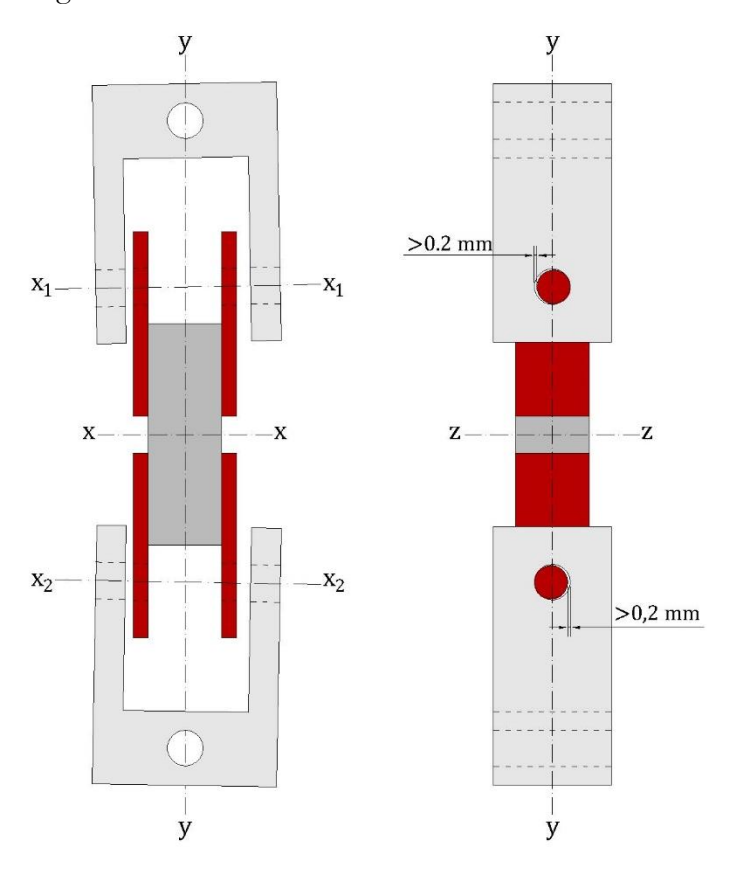


Figure 22 Device orientation while loading

From a geometric point of view, the advantage of the latter configuration is the possibility of obtaining a loading parallel to the longitudinal axis of the sample despite the geometric defects. This is because the first pivot allows the load to be applied to all four plates, while the second pivot allows the sample to align vertically. In addition, by leaving a greater clearance for geometric defects in the transverse plane between the loading axes and the holes of the U parts, the positioning of the sample is free (Figure 22).

Ultimately, this configuration improved the uniformity of loading across the cross section of the sample, with stray moments due to load application eccentricity being greatly reduced. Therefore, this loading device was chosen for the direct tensile tests.

Then, in order to evaluate the effect of the use of the adhesive assembly and of the bi-articulated loading device with 2 pivots, the statistical distribution of the forces at break of the cement paste samples was studied (Figure 23). This was done by comparing the results obtained from using these accessories with those obtained on the initial configuration.

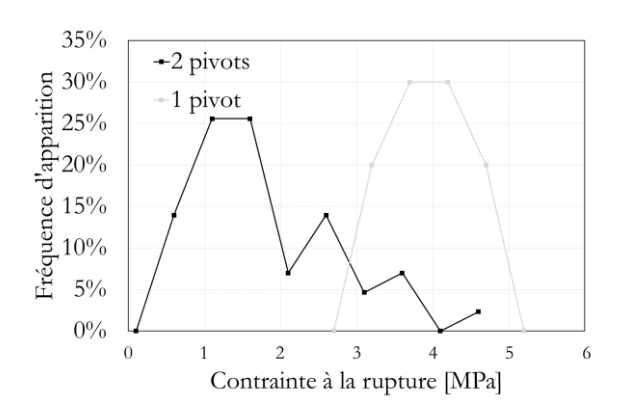


Figure 23 Statistical frequency of tensile rupture test in 2 different configurations

For the initial configuration, with 1 pivot and without adhesive assembly, a set of 50 samples was studied. A strong dispersion of the breaking stresses is observed with high frequency densities spread between 1 MPa and 4 MPa. For the second configuration with adhesive assembly and two pivots, a set of 10 samples was studied. We notice a monophasic statistical distribution which converges towards the average of 3.9 MPa. This value is brought closer to that which corresponds to another secondary frequency peak on the configuration with 1 pivot and without adhesive assembly, for a value of 3.6 MPa. However, for this configuration, only 15% of the values are concentrated around the peak of 3.6 MPa, while for the configuration with 2 pivots all of the values are located around the average of 3.9 MPa. Therefore, it can be concluded that the use of the glue fixture and the addition of a pivot resulted in a considerable improvement in repeatability on the breaking force of the paste.

In summary, a tensile test setup was implemented to track applied force, strain, and the occurrence of cracking of cement paste and paste / aggregate composites samples during stress. In this sense, in order to ensure satisfactory representativeness of the results obtained, additional accessories are used to standardize the mechanical stress during the test.

2.6. Conclusion

The mechanical behavior of sound or degraded concrete by leaching is influenced by the existence of ITZ which affects the properties of the paste / aggregate bond. However, the magnitude of this influence is difficult to estimate due to the difficulty of isolating the paste-aggregate bonds to study their properties. However, a more in-depth knowledge of the mechanical properties of these bonds is necessary to appreciate the mechanical behavior of concrete over the long term. Under these conditions, an experimental protocol was developed to analyze the influence of degradation on the mechanical properties of the paste / aggregate bond and on those of the paste.

In this sense, in order to assess the mechanical behavior of degraded concrete at the local scale of the paste / aggregate bond, the analysis of chemical degradation is necessary beforehand. As a result, several related aspects have been addressed in order to make the observations possible and representative. The overall aim is to prepare and condition samples with suitable configurations to allow analyzes at the microstructural scale and mechanical tests at the local scale. The measurement of the degraded thicknesses is intended to determine the degradation kinetics. As regards the mechanical tests, they are carried out to analyze the stiffnesses and strengths of the paste / aggregate bond and of the paste. An adaptation of the test devices at the local scale was carried out to extend the field of observation and increase the representativeness of the results.

The samples used for the analyzes envisaged are of parallelepiped shape, made of cement paste and paste / aggregate composites. In the area of interest, their cross sections are squares of 10x10 mm², allowing at this level the calculation of the progress of chemical degradation and the state of stress under mechanical stress. These samples were fabricated in flexible silicone molds in order to facilitate casting and demoulding, but also to minimize interference of the manufacturing method with measuring the properties of the samples. After fabrication, the samples were preserved in a water and lime bath for 40 days, to allow optimal hydration and prevent cracking. After the hydration period, a number of samples were individually subjected to accelerated unidirectional degradation in ammonium nitrate solution. The choice of this leaching method is justified by the high degradation rate and by the nature of the degradation scenario generated which is similar to the original scenario.

The degradation kinetics are defined as the change in degraded thickness over time, determined from image analysis of cross sections. The use of image analysis for the measurement of degraded thickness is facilitated by the contrast between the gray level of the degraded area and that of the sound area.

Mechanical tests were coupled with digital image correlation (CIN) for the calculation of displacements and strains. The displacement and deformation measurement by CIN was carried out using a high-resolution camera, with the objective of obtaining satisfactory precision of the local and global displacement and deformation fields. Using this method, stress / strain curves are obtained from which the mechanical properties of the samples are determined, as well as displacement and strain fields.

The direct tensile test is carried out on parallelepipedal samples of cement paste and composites. The principle of the test is to apply the tensile load to 4 plates bonded to 2 opposite sides of the sample, which are perpendicular to that observed by CIN. Particular attention was paid to this tensile test, with the aim of improving and standardizing the experimental loading conditions. The strategy adopted was that of controlling the boundary conditions imposed on the samples through the realization of a bonding assembly of the loading plates and the use of a bi-articulated loading device. The assembly of the adhesive was designed to minimize geometric defects and guarantee satisfactory parallelism of the loading axes. Subsequently, the bi-articulation of the loading device helped to even out the distribution of the load to the loading plates, minimizing the effect of geometric defects in the bonding. These two measurements thus allowed a significant improvement in the repeatability of the results.

By taking stock of the aspects presented, this experimental protocol has a basic vocation, that of allowing the evaluation of the effect of leaching on the mechanical behavior of concrete on a local scale.

3. Results and discussion

The mechanical properties of concrete degraded by leaching depend on the phenomena that occur at the local scale of the paste / aggregate bond. However, an exploration on this scale requires an experimental methodology oriented towards the link which exists between the chemical degradation and the mechanical properties of the material. In this sense, an experimental protocol was defined in the previous chapter. Therefore, in this chapter, the results obtained using this experimental protocol will be presented. In order to support these results, and due to a particular

experimental methodology, the use of related experimental methods allows the verification of the results obtained.

First, the degradation kinetics of the samples is analyzed. The basic objective is to determine, for several degradation times, the rate of chemical degradation of ITZ and cement paste which is a characteristic variable for the progress of degradation.

In order to access the mechanical properties of the paste / aggregate bond and the paste, local mechanical tests are first performed on sound samples. The mechanical properties are obtained through stress / strain curves, while additional information is revealed by the displacement and strain fields.

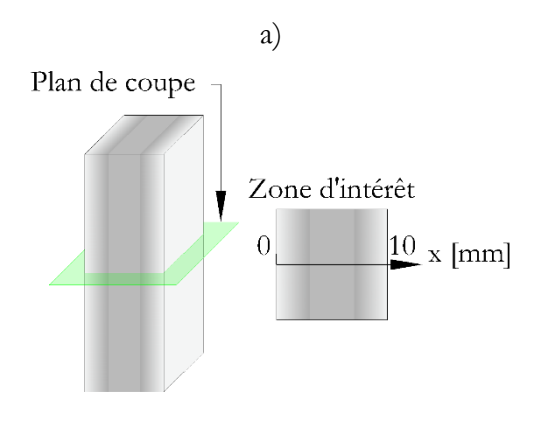
After this step, the effect of chemical degradation on the mechanical properties of the aggregate paste and paste bond is evaluated in relation to the rate of chemical degradation.

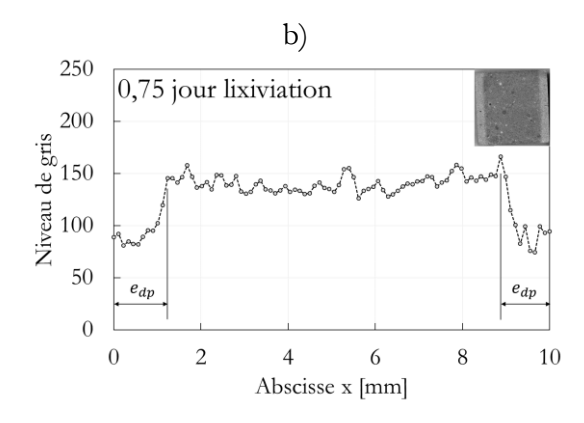
3.1. Leaching kinetics

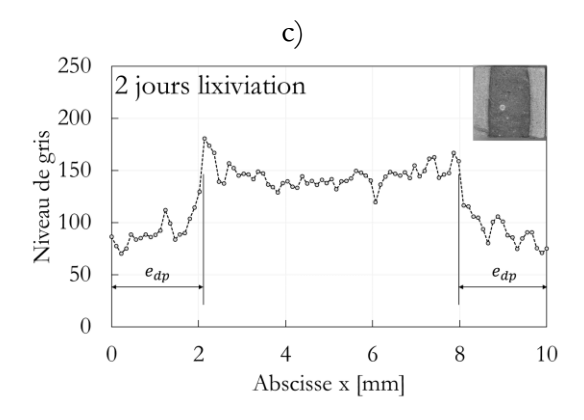
The measurement of the degraded thickness was carried out following the analysis of the evolution of the gray level on the cross section. This was made possible by the obvious contrast between the gray level of the degraded areas at the ends of the cross section and the sound area in the middle.

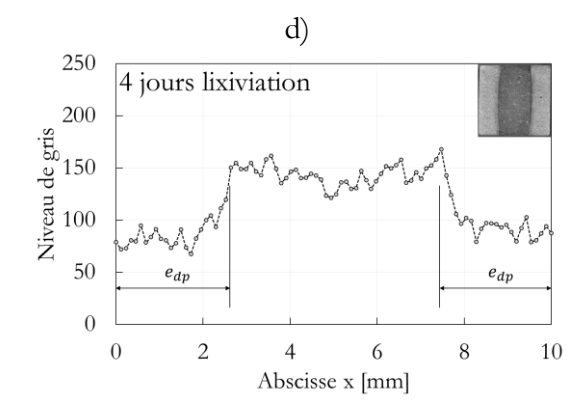
The gray level profiles were plotted along the median of the cross section, according to the method presented in paragraph 2.4. On these gray level profiles, the measurement of the degraded thicknesses of the e_{dp} paste and at the e_{di} interface was possible thanks to the delineation of the sounf and degraded areas.

Images of the cross-sections of the cement paste samples, along with the associated gray level profiles, each degradation time are shown in Figure 24.









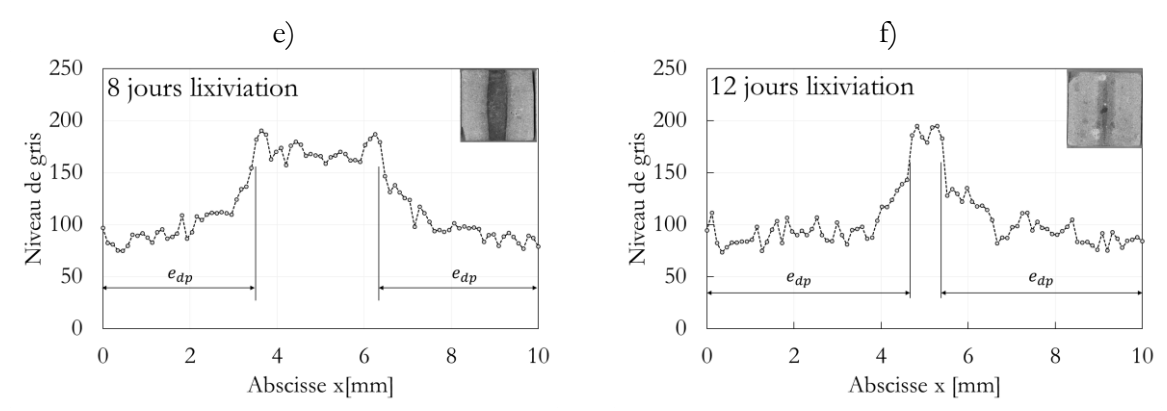


Figure 24 Gray level evolution on the median of cement paste sample cross section. Measurement principle(a); Samples after 0,75 day (b), 2 days (c), 4 days (d), 8 days (e) and 12 days (f) of leaching

In this figure, we see that the gray level is high in the sound area while it is lower in the degraded area. In the degraded zone, there is an intermediate zone where the decrease in the gray level is rapid and varies between the high value encountered in the sound zone and the reduced value encountered at the end of the degraded zone.

Once the measurement of the degraded thicknesses obtained by image analysis carried out, it was possible to determine the degradation kinetics through the relationship between the degraded thickness and the square root of time, illustrated in Figure 25. In this figure, we observe that the evolution of the degraded thickness as a function of the square root of time can be approximated by a straight line. The proportionality of the degraded thickness with respect to the square root of time is a consequence of the diffusive nature of the leaching kinetics in ammonium nitrate solution (Carde et al., 1996; Mainguy et al., 2000; Nguyen, 2005). In our case, we can approach the value of the degraded thickness of the paste e_{dp} as a function of time by:

$$e_{dp} = 1.35 * \sqrt{j} \tag{3.1}$$

où j est la durée de dégradation exprimée en jour.

Thanks to the knowledge of the degraded thickness, it is necessary to define the state of progress of the degradation by a variable which can be associated with the evolution of the mechanical properties. This variable is represented by the chemical degradation rate $\delta_{P\hat{a}te}(t)$, calculated for each degradation time t, and defined as the ratio between the area of the degraded surface of the cross section $A_{d\,P\hat{a}te}(t)$ and the total area of the cross section A_t :

$$\delta_{P\hat{a}te}(t) = \frac{A_{d\ P\hat{a}te}(t)}{A_t} = \frac{2 * e_{dp}(t) * l}{l^2} = \frac{2 * e_{dp}(t)}{l}$$
(3.2)

where $e_{dp}(t)$ represents the degraded average thickness measured for a given degradation time; l represents the dimension of the square cross section of 10 mm.

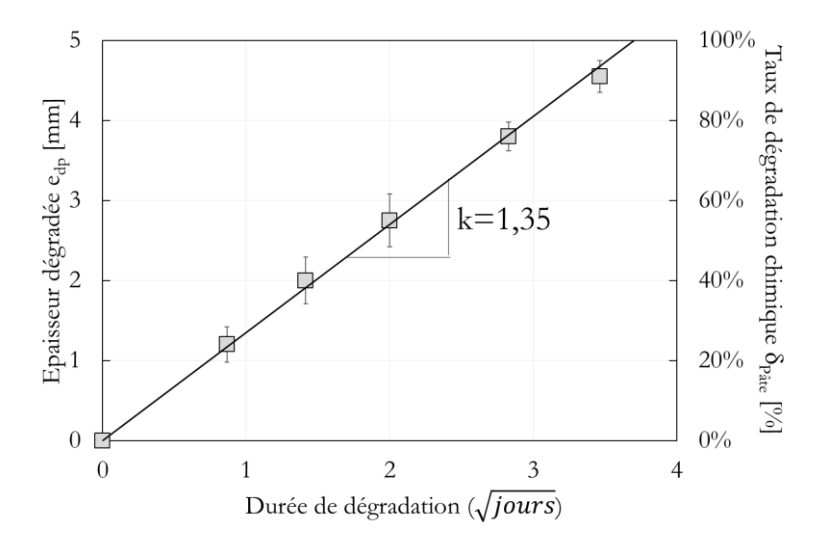
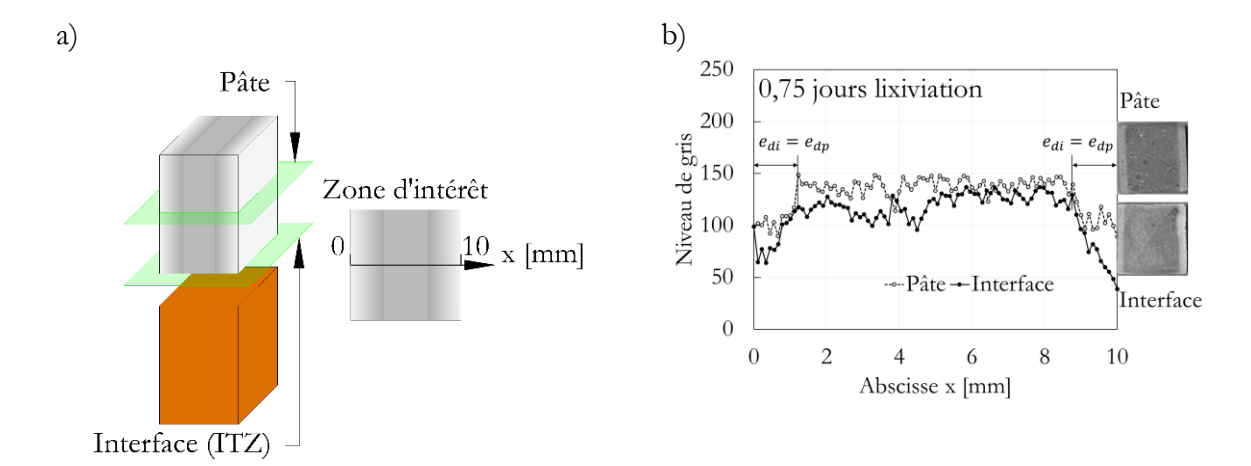


Figure 25 Leaching kinetics of cement paste

Regarding the proportionality factor between the degraded thickness and the square root of the degradation time expressed in days, its value is 1.35. This value is substantially similar to that obtained by Carde (Carde and François, 1997a) on cement paste cylinders (diameters between 10 and 30 mm) with a similar chemical composition: pure Portland cement CEM I and w / c of 0, 4. On the other hand, this proportionality factor is less than 2, a value obtained by Jebli (Jebli, 2016) who used a similar degradation protocol but on a more diffusive material: CEM II cement paste with w / c of 0.5. Other larger proportionality factors have been obtained by researchers who have used additional means of acceleration, such as continuous agitation (Heukamp, 2003; Le Bellégo, 2001).

Following the measurement of the degraded thicknesses on paste samples, the degraded thicknesses were also measured on composite samples. For these composite samples, the gray level profiles obtained at the interface and at the core of the cement paste for different degradation times are presented in Figure 26. The method by which these profiles were obtained is presented in the paragraph 2.4.

In this figure, it is generally observed that by increasing the degradation time, the degraded thicknesses measured at the interface and in the cement paste increase. However, over time the degraded thickness measured at the interface begins to become greater than that measured in the paste.



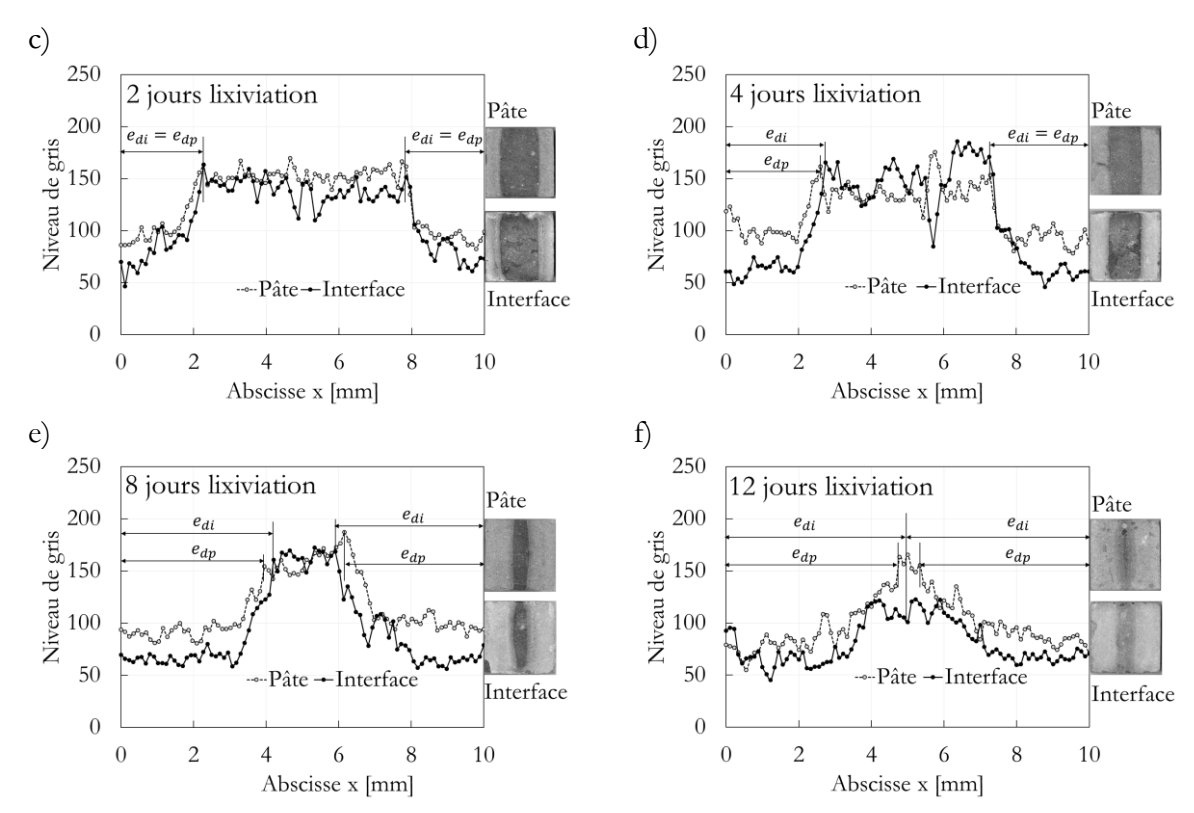


Figure 26 Gray level evolution on median of composites samples cross section at interface and within bulk cement paste. Measurement principle (a); Composites samples after 0,75 day (b), 2 days (c), 4 days (d), 8 days (e) et 12 days of leaching (f)

The degraded thickness measured at the e_{di} interface was considered representative for the ITZ, as it was measured at the interface. From this degraded thickness of ITZ, the chemical degradation rate of ITZ, δ_{ITZ} was calculated in a manner analogous to that of paste (relation (3.2)). The degraded thickness measured at the paste core on composite samples is similar to that measured on pure paste samples.

Subsequently, in order to assess the relative change in the rate of chemical degradation of ITZ compared to that of the paste, the ratio between these two quantities was calculated for each composite sample. Therefore, in Figure 27, the evolution of this average relative ratio is represented as a function of the average degradation rate of the paste associated with the same degradation time.

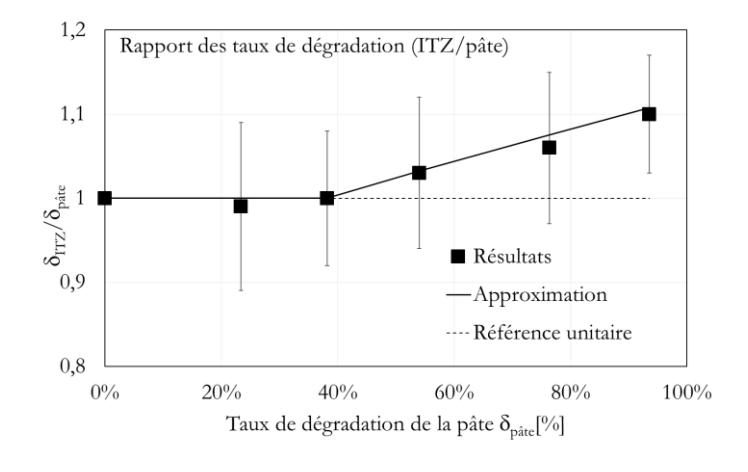


Figure 27 Evolution by time of degradation rate of interface and of cement paste

In this figure, it can be seen that in the field of degradation rates below 40%, the ratio between the chemical degradation rate of ITZ and that of the paste is almost unitary. For chemical degradation rates greater than 40%, the degradation kinetics of ITZ accelerate to a maximum ratio of approximately 1.1. Indeed, at this time, the ITZ is completely degraded (Figure 26), while, in the heart of the cement paste, we still notice a sound zone.

During all the observations made in this paragraph, the modeled chemical degradation kinetics of paste and ITZ are presented in Figure 28. This degradation kinetics is represented by the time course of the chemical degradation rate. The rates of chemical degradation of ITZ and paste coincide at the start and are proportional to the square root of time. The acceleration of the degradation kinetics of ITZ is a consequence of the increased diffusivity. This phenomenon occurs initially as a result of the significant increase in porosity generated by the dissolution of portlandite at the degraded ITZ. Another factor that can further accelerate the degradation kinetics of ITZ is interface cracking. In fact, from 8 days of leaching, the samples become pre-cracked, following chemical degradation. However, the additional effect of cracking on accelerating the degradation kinetics of ITZ is not significant.

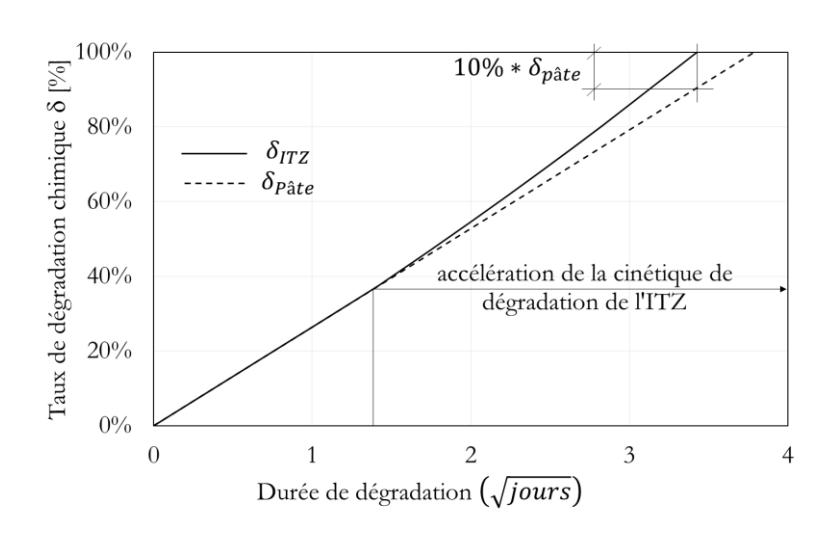


Figure 28 Modelized leaching kinetics of ITZ and cement paste

3.2. Leaching effect on mechanical behaviour of concrete at local scale

In this subsection, the effect of leaching on the mechanical properties of cement paste and cement paste / aggregate composites was investigated in support of tensile testing. The effect of chemical degradation on the stiffness and strength of the samples will be evaluated through stress / strain curves. This analysis will be supplemented by a discussion of the influence of the cracking which is observed on these degraded samples. In this sense, for each degradation rate associated with the 5 degradation times, 10 cement paste samples and 10 composites were analyzed.

It is mentioned that the vertically cast composite samples were used for testing due to a stronger paste / aggregate bond than in the case of horizontally cast composites. The choice of this type of composite made it possible to preserve sufficient adhesion between paste and aggregate for high degradation rates, in order to be able to observe the loss of adhesion at the interface over a sufficiently large area.

3.2.1. Evolution of mechanical properties

In order to access the stress / strain curves representative of the samples, the orientation of the samples with respect to the camera was chosen to allow uniform stress on the sound and degraded areas. With this in mind, Figure 29 shows the orientation of the faces of the degraded samples observed by correlating digital images during tensile tests.

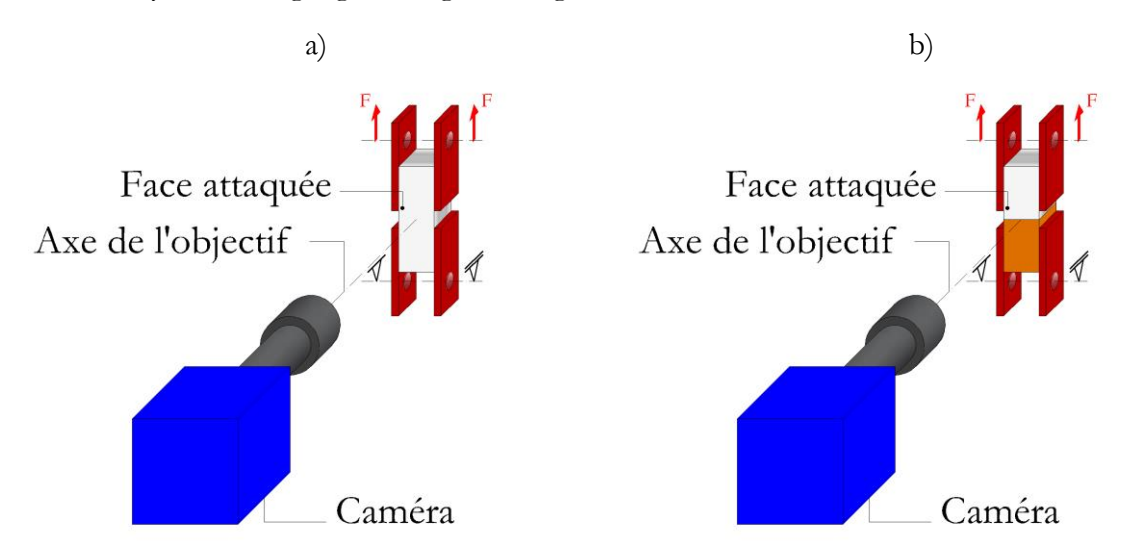


Figure 29 Orientation of cement paste a) and composite b) samples while tensile test

On the degraded samples, measurements of displacements and deformations by CIN were carried out on an attacked face which was in contact with the aggressive solution. As for the loading plates, they were glued on a face parallel to the direction of degradation. This results in parallel loading of the sound zone and the two degraded zones located on one side and the other of the sound zone. Therefore, in this configuration, the face observed by CIN is the one that has undergone the most significant chemical degradation. However, due to the parallel loading of the sound and degraded areas, the deformations measured on this face are representative for the entire sample.

Following the use of this configuration for loading and observation of deformations, stress-deformation curves were obtained. Stresses and strains were calculated in the same way as for sound samples, according to the relationships. Figure 30 shows stress / strain curves of cement paste and composite samples for different degradation rates. Unlike the sound samples for which the stress / strain curves were obtained by linear approximation, those of the composite samples were determined by polynomial approximation from the raw curves. The choice of this type of approximation is justified by the changes in the slopes which are observed on these curves.

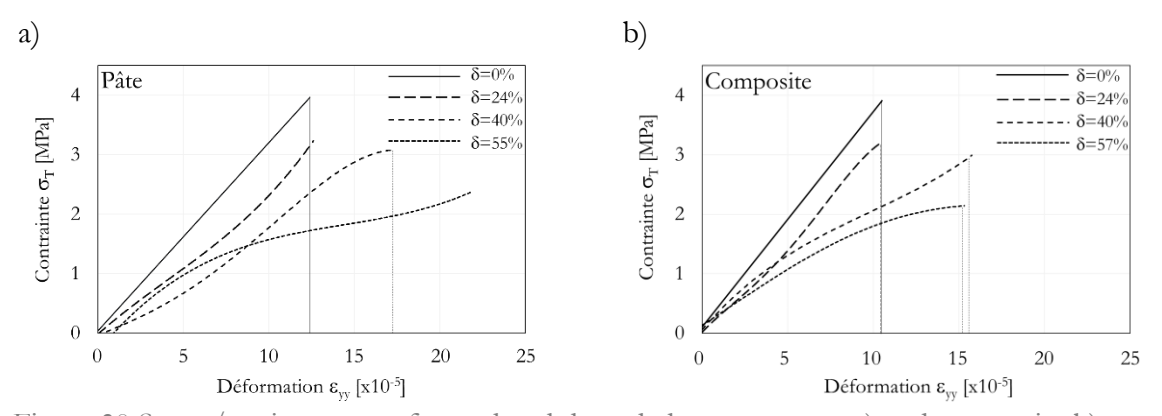


Figure 30 Stress/strain curves of sound and degraded cement paste a) and composite b) samples

On these stress / strain curves, we observe, in the broad sense, that the samples become less resistant and less rigid when the degradation rates increase. For degraded samples, their stress / strain curves show non-linear portions of the curve, the extent of which increases with increasing degradation rate. The nonlinear part manifested by the softening of the curve is a consequence of cracking. This aspect will be discussed in paragraph 3.2.2.

Taking into account the broader objective of evaluating the mechanical behavior of degraded samples, firstly the evolution of the Young's modulus of the paste and of the composite as a function of the chemical degradation rate was analyzed.

The Young's modulus of the samples was obtained in the pre-cracking part of the stress / strain curves, where the behavior is assumed to be linear elastic. Such an example of a curve is shown in Figure 34.

Following the determination of the Young's moduli of the samples, their evolution as a function of the rate of chemical degradation is presented in Figure 31, for the paste and for the composite.

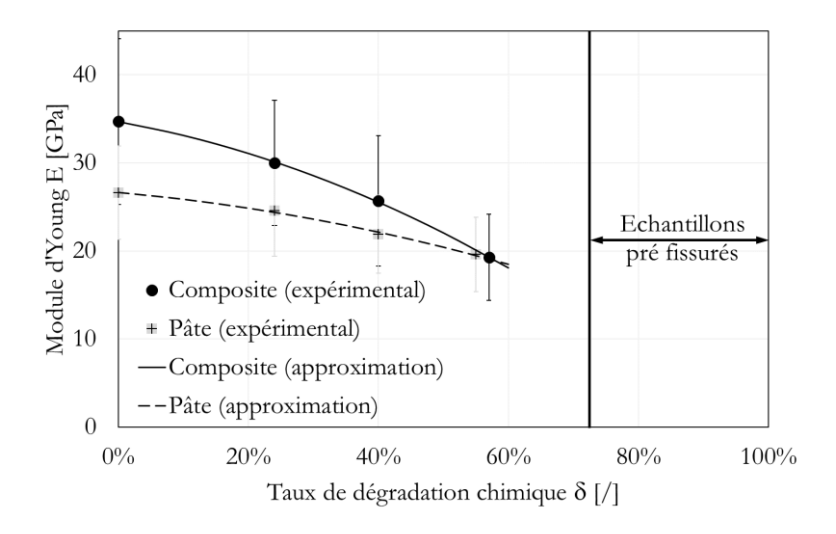


Figure 31 Young modulus evolution of cement paste and composite as a function of chemical degradation rate

In this figure, the evolution of Young's moduli of cement paste and composite samples were approximated by polynomial curves. This is a similar approach to that used by other authors in the literature (Carde and François, 1997a; Le Bellégo, 2001; Nguyen, 2005) who have studied the evolution of the mechanical properties of cementitious materials (paste, mortar or concrete), in compression or in bending. These authors generally find a linear evolution of rigidity and resistance as a function of the rate of degradation at different scales (from 10 mm cylinders to 40x320 mm beams in section). In our case, the evolution of the Young's moduli of the samples was approximated by polynomial curves, because the decreasing slope is accentuated by increasing the rate of degradation.

The changes in the Young's moduli of the paste and the composites were obtained for chemical degradation rates of up to 57%. For higher degradation rates, the Young's modulus was no longer measured because the samples were pre-cracked before loading. This pre-cracking occurs either in the paste or at the paste / aggregate interface in the case of composite samples. According to the literature, pre-cracking due to chemical degradation occurs as a result of the development of pre-stress generated by the shrinkage of the paste. This phenomenology has been observed and analyzed in more detail by (Burlion et al., 2007; Rougelot et al., 2010). In fact, as a result of

endogenous shrinkage and decalcification shrinkage of the paste, stress concentrations build up during leaching between the sound zone and the degraded zone of the paste and at the interface between the cement paste and the aggregate. Once these stresses exceed the tensile strength of the degraded material, cracks open.

In the same figure, we observe that the decrease in the Young's moduli of the composite is more pronounced compared to the cement paste, but the values of the Young's moduli of the composite are higher than those recorded for the paste. However, a direct comparison between these two quantities is not relevant, because the composite contains an aggregate half, which is not affected by leaching during the duration of the study, in accordance with the observations carried out by Jebli (Jebli, 2016).

Under these conditions, in order to be able to evaluate the influence of ITZ on the loss of rigidity of the cement paste / aggregate bond, it was decided to refer to the case of a perfect bond. The model with two springs linked in series (paste and aggregate) makes it possible to calculate the equivalent modulus of elasticity of the composite under the assumption of perfect contact for each level of degradation. This imaginary modulus of the ideal composite with perfect bond was calculated based on the rate of chemical degradation. For a given chemical degradation rate δ , the Young's modulus of the ideal composite $E_{cp}(\delta)$ was calculated from the modulus of the paste corresponding to the same chemical degradation rate $E_p(\delta)$ and the Young's modulus of the aggregate E_q following a reasoning similar to that which was presented in the chapter:

$$E_{cp}(\delta) = \frac{1}{\frac{1}{E_p(\delta)} + \frac{1}{E_g}}$$
(3.3)

After the calculation of the Young modulus of the ideal composite by this formula, the evolutions of the Young modulus of the ideal and real composites are shown in parallel in Figure 32. In this figure, we observe that the Young modulus of the composite actual is lower than that of the ideal composite for the observed degradation rates. Following leaching, the difference between the Young's moduli of the two composites increases, indicating significant degradation of the actual cement paste / aggregate bond. Indeed, the difference between the Young's modulus of the ideal composite and that of the real composite comes from the flexibility of ITZ, as well as from its significant chemical degradation. In a sound state, the chemical composition of ITZ makes the paste / aggregate bond less rigid compared to paste due to the high concentration of portlandite. This chemical species has cohesive properties inferior to the C-S-H which are predominant in the paste core. Then, in the degraded state, following the total dissolution of the portlandite, the rigidity of the cement paste / aggregate bond is more affected than that of the cement paste, due to the significant increase in porosity.

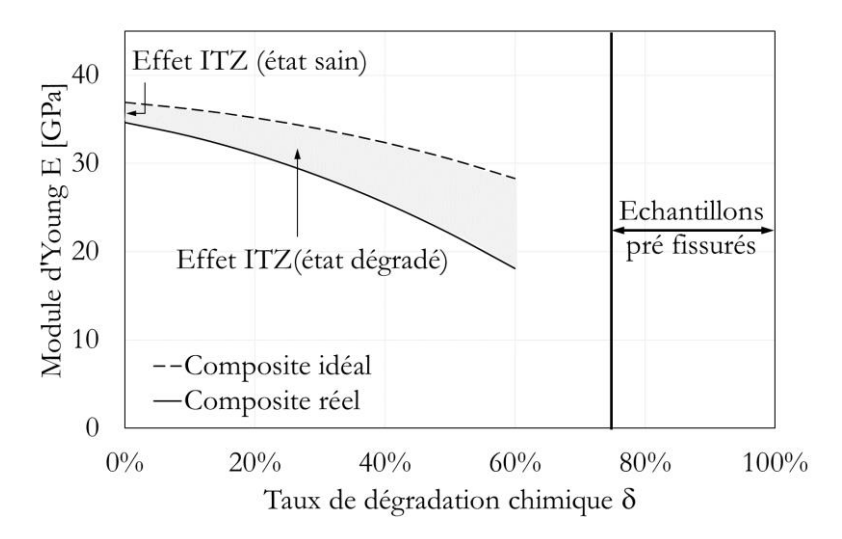


Figure 32 Evolution of Young modulus of equivalent ideal (perfect bond) and real composite

As part of the study of the mechanical properties of degraded samples, after the Young's modulus, we focused on the breaking stresses. In this sense, the evolution of the tensile strength of paste and composite samples as a function of the chemical degradation rate is illustrated in Figure 33.

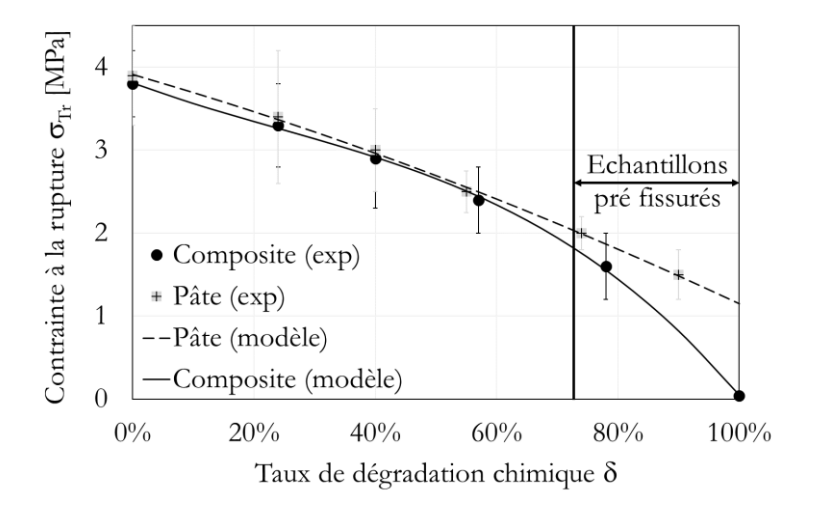


Figure 33 Evolution of tensile stress at rupture (breaking stress) as a function of chemical degradation rate

In this figure, the evolution of the breaking stresses as a function of the degradation rate is approximated by polynomial curves. In the case of paste samples, this evolution is almost linear. This type of evolution is consistent with those from other works in the literature that have looked at the mechanical behavior of leached cementitious materials (paste, mortar or concrete), but on a macroscopic scale. Several authors (Carde and François, 1997b; Le Bellégo, 2001; Nguyen, 2005) have found a linear dependence between the mechanical strength and the rate of chemical degradation for various types of tests (compression and bending).

On the other hand, in the case of composites, two tendencies can be delimited. For chemical degradation rates of less than 60%, the breaking stresses of the composites are almost equal to those of the paste, because the rupture of the composites occurs preferentially in the paste. Then, the breakdown of composites begins to occur at the interface and the nominal tensile stress drops to near zero at a chemical degradation rate of 100%.

These different evolutions of the breaking stresses, observed for the paste and composite samples as a function of the chemical degradation rate are influenced by the cracking which appears during loading or before this one. In this sense, the influence of cracking on the mechanical behavior of samples is discussed in the next paragraph.

3.2.2. Observation of cracking

The observation of the cracking of the samples was possible thanks to the study of the displacement fields. On these fields, the cracks, by the effect of their openings, appear as local discontinuities.

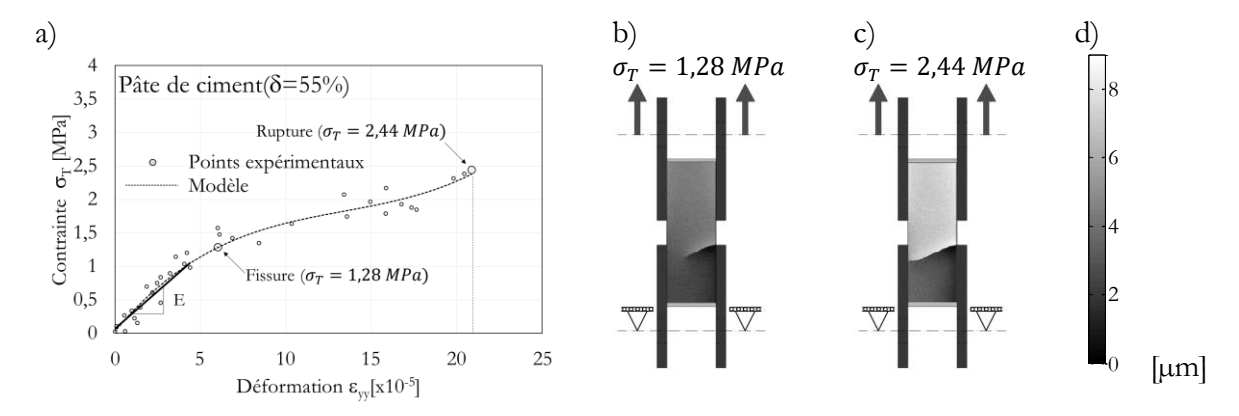


Figure 34 Illustration of cracking effect on stress/strain curves. Stress/strain curve a), vertical displacement field after crack onset b) and before rupture c)

Therefore, in order to be able to assess the effect of cracking on the mechanical properties of the samples, the stress / strain curves were compared with the displacement fields. Figure 34 shows a stress / strain curve of a paste sample for a degradation rate $\delta = 56\%$, as well as the displacement fields after crack opening and before failure. The same figure also illustrates how to obtain the Young's modulus from the linear part of the curve, the pre-cracking.

In this figure, we observe that the appearance of the crack on the observed face results in the softening of the slope of the stress / strain curve. This phenomenon is observed on some of the degraded samples. On the rest of the samples, the stress / strain curves show a change in slope in the other direction. After the linear part, the slope becomes steeper or even changes direction. On these samples, probably the cracking appears on the posterior surface, not observed.

In order to provide an image of the different types of cracks that are observed on the paste samples, in Figure 35 three displacement fields at the instant before failure of the 3 different samples for a degradation rate of 57% are shown.

In this figure, it is observed that the location and the shape of the cracks are quite variable, but in a preferential zone, that located generally between the upper plates and those lower. The majority of cracks appear in the proximity of the junctions with the plates due to the stress concentrations that develop there. A smaller, but significant amount of cracks is noted in the middle area. The appearance of cracks in this area probably occurs in response to the existence of local defects in the structure of the material.

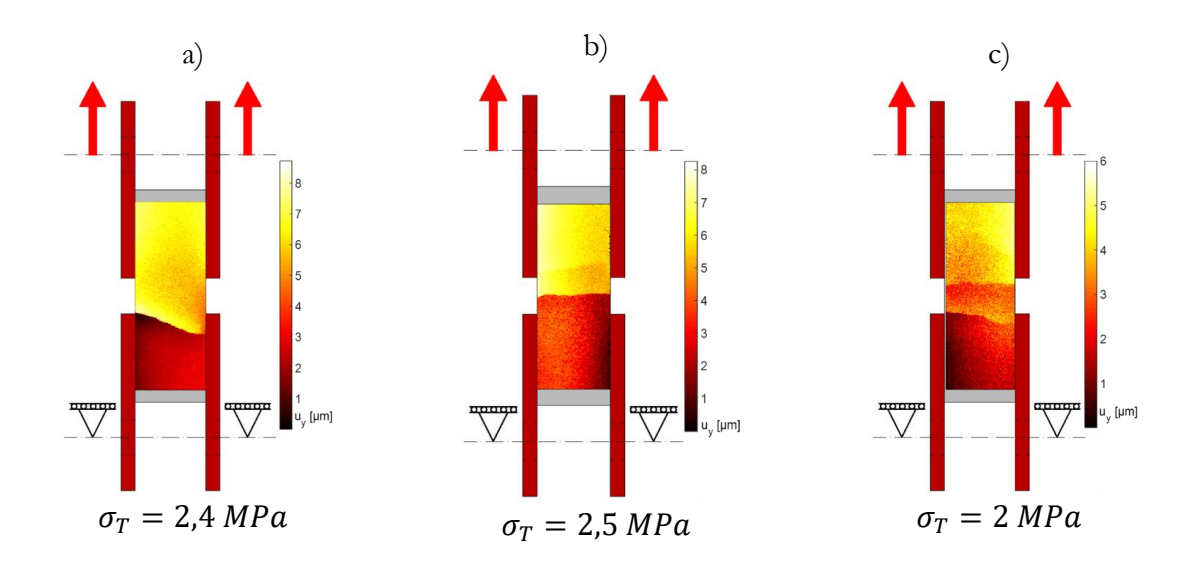


Figure 35 Displacement field examples of cracked cement paste samples

Subsequently, taking into account that for the paste samples where the cracks were visible on the observed face, the stress at the time of the opening of the crack can be identified, it was recorded as the stress at cracking σ_{Tf} .

In order to assess the influence of cracking on the breaking stress of the paste, Figure 36 shows the evolution of the breaking stress and the cracking stress as a function of the rate of chemical degradation. By comparing the two curves, we notice that the stress at cracking drops more quickly and even reaches zero, for the degradation rate for which the samples become pre-cracked before loading. It should be noted that despite a faster decrease in the stress at cracking, the decrease in the stress at break does not accelerate significantly and keep an almost linear appearance.

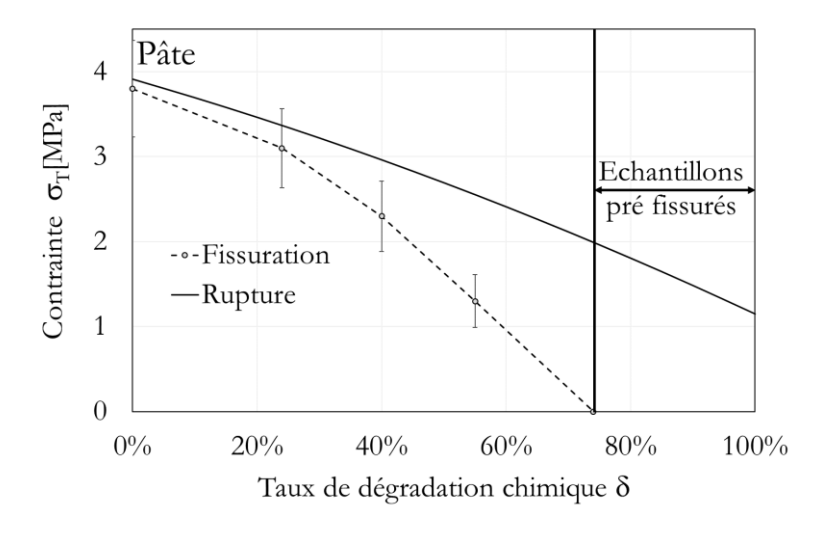


Figure 36 Evolution of stress at cracking of cement paste

This behavior of the cement paste is quite particular, because generally in tension, cementitious materials exhibit rapid rupture after opening of the cracks (Bažant and Cedolin, 1993; Mier and Vliet, 2002; Swaddiwudhipong et al., 2003; Zhou, 1988). This is because after opening the cracks, the cross section decreases, and a redistribution of stresses occurs. Then, the loading becomes eccentric and the final rupture is accelerated. Nevertheless, this type of behavior has been observed on undegraded materials, but for loading configurations similar to those used in the present study.

However, in our case, cracking is observed in the degraded part. Indeed, the origin of the significant residual resistance after the opening of cracks in the degraded area is in the way of loading this area. In the present study, the test configuration involves parallel loading of the sound zone and the degraded zones which can be modeled by springs (Figure 37a). During such parallel loading, considering perfect bonding with the loading plates, the deformations of the various springs associated with the sound and degraded areas are equal. Therefore, the force supported by each spring is proportional to its stiffness. In the case of this test, the cracks observed are found on the filmed side, the side which was in contact with the aggressive solution, and therefore the most chemically degraded area. The spring that corresponds to this zone supports a reduced part of the total load, since it is proportional to its reduced rigidity. Therefore, the redistribution of stresses which appeared following cracking has a reduced magnitude and is not sufficient to generate a significant eccentricity of the loading (Figure 37 b). Apart from this, degraded CEM I cement paste exhibits greater deformability than sound paste (Heukamp et al., 2003), which can delay the propagation of the crack in depth. All these aspects combined can indeed result in limiting cracking to a surface area until the approach of final failure. This explains the significant strength of the samples after crack opening.

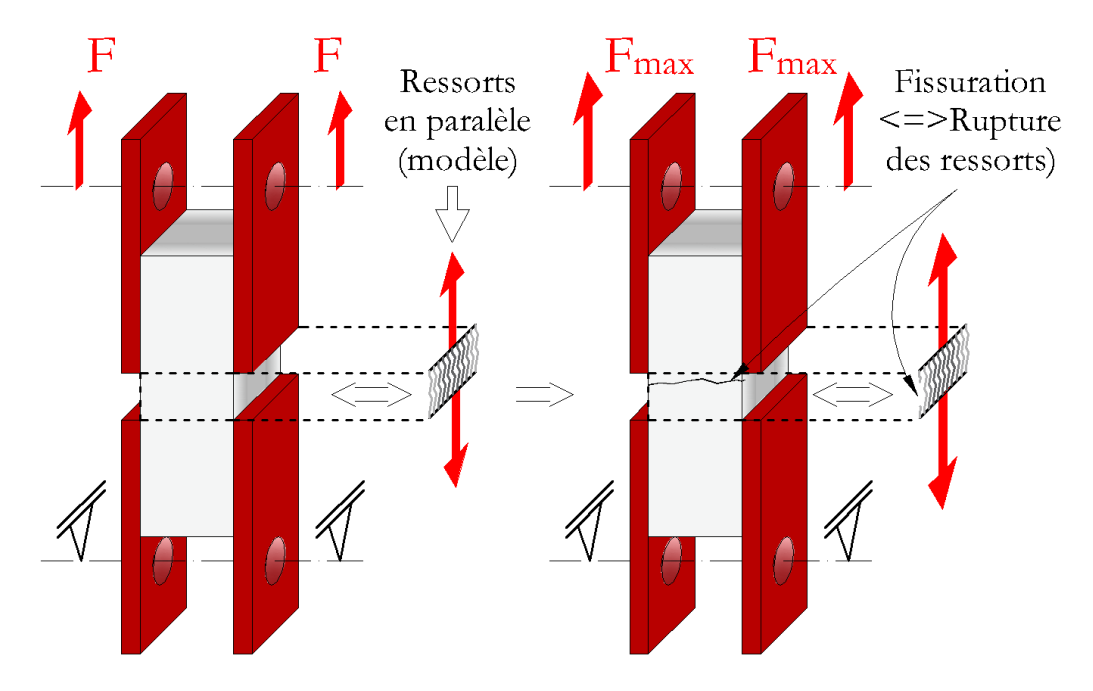


Figure 37 Illustration of loading and cracking of cement paste sample

After interpreting the influence of cracking on the behavior of paste samples during tensile testing, the same type of discussion will be conducted for composites. In the case of composites, the notion of stress at cracking is irrelevant to characterize the paste / aggregate bond, because cracks occur not only at the paste / aggregate interface, but also in the paste. However, a significant number of samples show interface cracks and this number has been recorded. Figure 38 shows a displacement field of a composite sample cracked at the interface prior to failure. Unlike cracks in cement paste, interface cracks appear across the width of the interface and their opening increases until failure.

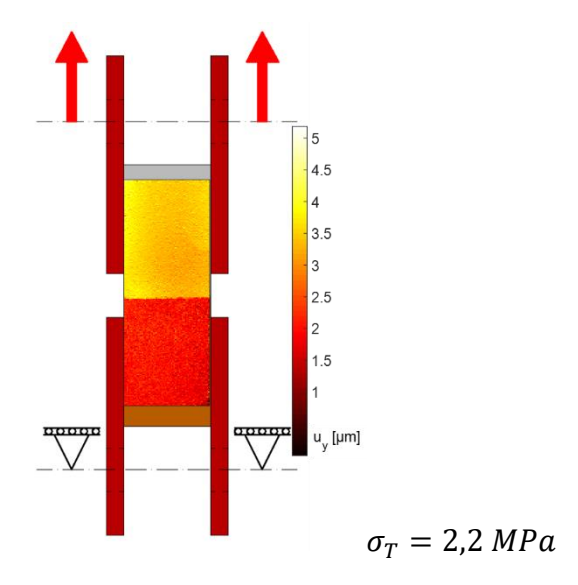


Figure 38 Displacement field of a cracked composite sample

For composite samples, only the frequency of appearance of cracks at the interface was counted. For a given degradation rate, the frequency of appearance of cracking at the interface of composites was considered equal to the ratio between the number of samples on which cracks at the interface were observed and the total number of samples. Some samples that show interface breaks do not show interface cracks visible on the displacement fields prior to failure. In the case of these samples, probably the cracking which precedes the rupture occurs on the face opposite to that filmed. In fact, it is possible that the frequency of appearance of cracking at the interface measured in this way is lower than the real proportion of samples cracked at the interface, because the cracks which appear on the face opposite to that observed are not visible. However, in order to offer a rather qualitative overview of the occurrence of cracking at the interface, Figure 39 presents the evolution of the frequency of appearance of cracks at the interface of composite samples as a function of the degradation rate. chemical. In the same figure, the change in the frequency of occurrence of breaks at the interface of composites as a function of the rate of chemical degradation is also presented.

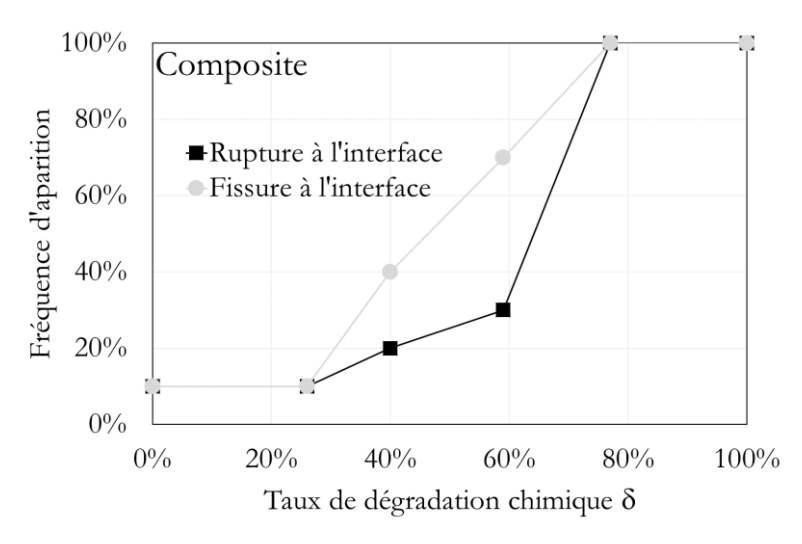


Figure 39 Evolution of ratios of composite samples cracked and broken at interface

In this figure, we can see that on sound samples and with a chemical degradation rate less than or equal to 24%, the rate of appearance of cracking and rupture at the interface is limited to 10%. Then, the rate of occurrence of cracking and rupture at the interface increases to 100% for a

chemical degradation rate of 76%. The faster growth in the occurrence of cracking is explained by the fact that some of the samples show cracks at the interface but breaks in the paste.

In order to assess the behavior of the cement paste / aggregate bond subjected to leaching, Figure 40 offers a global picture of the loss of adhesion as a function of the rate of chemical degradation. Consequently, in this figure, several characteristic quantities for the mechanical behavior of the paste / granulate bond are represented, but which are also linked to that of the paste. This is the ratio between the Young's modulus of the real composite and that of the ideal composite, the ratio between the tensile stress of the composite and that of the paste, as well as the frequency of occurrence of the break at the composite interface.

In this figure, we observe that the loss of adhesion is progressive and manifests itself simultaneously on the three quantities concerned.

At first, for chemical degradation rates below 24%, the quality of the cement paste / aggregate adhesion was rated as "good". In this step, the loss of Young's modulus is limited and the breaking of the composites occurs in the paste in 90% of cases for stresses similar to those encountered for the samples in paste.

Then, for chemical degradation rates between 25% and 60%, a decrease in the adhesion between the cement paste and the aggregate begins to be felt. The decay of the Young's modulus of the real composite accelerates, while the frequency of occurrence of breaks at the interface of composites increases. However, the nominal tensile stress values of composites remain close to those of the paste.

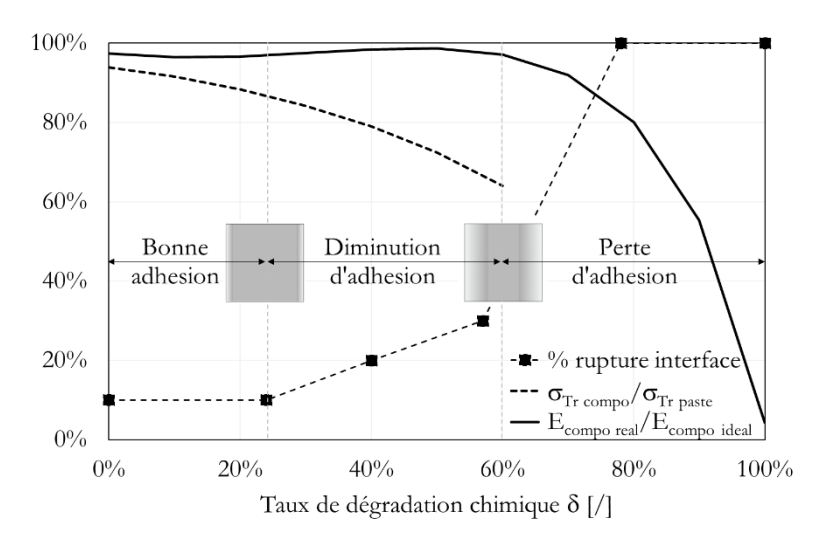


Figure 40 Adhesion loss of cement paste /aggregate bond as a function of chemical degradation rate

Finally, for chemical degradation rates greater than 60%, pre-cracking before loading is observed at the paste / aggregate interface, while the breakdown of composites occurs at the interface for stresses lower than those of the paste. The loss of adhesion is complete for a chemical degradation rate of 100% when the tensile strength of the composite is minimal.

Subsequently, a comparison can be made between the results obtained in this study and those obtained by Jebli (Jebli et al., 2018) which carried out a test campaign on paste and composite samples at the same scale. The difference between this study and the present one was that Jebli used a formulation specific to ordinary concrete: CEM II LL 32.5 cement, w / c ratio of 0.5 and

limestone aggregates. In the case of his study, the breaking stresses of the paste samples (2.4 MPa in the sounf state) and composites (1.7 MPa in the sounf state) were visibly lower compared to those obtained in the present study, while all of the composites exhibited interface breaks. Another important difference has been noticed in the evolution of mechanical properties. A large drop in Young's modulus and tensile stress was observed for reduced chemical degradation rates, but this trend subsided for greater chemical degradation rates. Therefore, by comparing the results of the two studies, it is observed that the use of a cement with a higher strength class and the reduction of the w / c ratio had a beneficial effect on the quality of the paste / aggregate bond subjected to leaching.

3.2.3. Conclusion

This section has demonstrated the nature of the effect of chemical degradation by leaching on the mechanical properties of cement paste and paste / aggregate composites on a local scale.

Differences that were noted between the chemical degradation of cement paste and that of ITZ were reflected in the mechanical behavior of the cement paste samples and composites. The chemical degradation of ITZ was more pronounced than that of the cement paste core due to the strong chemical dissolution of portlandite which is present in excess in sound ITZ. The strong dissolution at the ITZ level resulted in a significant increase in porosity which had generated a slight acceleration in the degradation kinetics.

Regarding the mechanical behavior, the leaching generates a significant decrease in the Young's modulus and the tensile stress of composites. Among other things, this is mainly a consequence of the significant chemical dissolution that occurs in the ITZ. The decrease in the mechanical properties of the composite is greater than that of the paste and culminates in a complete loss of adhesion of the interface in the degraded zone.

Additionally, the beneficial effect of using cement with higher strength class and lowering the w / c ratio has been shown. An important difference was noticed between the mechanical behavior of the samples (in paste and composites) made with a typical formulation of high performance concrete and another of ordinary concrete.

4. General conclusions

In this study, microstructural scale analyzes and local mechanical tests were used to interpret the mechanical behavior of the paste and of the paste / aggregate bond. The strategy adopted was to evaluate the effect of ITZ on the mechanical behavior of the cement paste / aggregate bond in a sound and degraded state, taking the cement paste as a reference.

The first aspect was the degradation kinetics of the cement paste and ITZ, due to measurement of degraded depth (thickness) by image analysis for several degradation times. This allowed the calculation of chemical degradation rates, used as a characteristic variable for the chemical degradation state. Due to the diffusive nature of the propagation of chemical degradation, the paste degradation kinetics is proportional to the square root of time. In contrast, that of the ITZ initially coincides with that of the paste, but accelerates slightly after a critical threshold to reach a maximum relative difference of 10%. The acceleration of the degradation kinetics of ITZ relative to the paste is probably a consequence of the increased diffusivity generated by the large porosity that formed as a result of the chemical dissolution of portlandite.

With regard to the tensile tests, through them, the evolution of the mechanical behavior of the samples was analyzed as a function of the chemical degradation rate. This chemical degradation rate is the ratio of the area of the degraded zone to the total area of the cross section. In terms of rigidity, the influence of ITZ materialized by the weakening of the paste / aggregate bond which becomes more pronounced following chemical degradation. This aspect is revealed by the evolution of the Young's modulus of the composite as a function of the chemical degradation rate, which undergoes a greater decrease than that of the paste because of the significant dissolution in the ITZ. With regard to the stresses at rupture, it has been observed that those of the composites decrease more rapidly as a function of the rate of chemical degradation than those of the paste. For the paste samples, the evolution of the tensile stress shows an almost linear dependence on the rate of chemical degradation, which is probably favored by shallow cracking. In contrast, for composite samples, the average stress at rupture is close to that of the paste up to a certain critical degradation rate. This critical chemical degradation rate corresponds to the onset of pre-cracking and the location of ruptures at the paste / aggregate interface. After this critical degradation rate, the loss of tensile stress in composites accelerates more than that of the paste, possibly due to a greater depth of cracking. Finally, the loss of paste / aggregate adhesion is complete when the ITZ is completely degraded.

Therefore, the main conclusion concerns the mechanism by which the ITZ transition zone influences the behavior of the degraded paste / aggregate interface after leaching. First, an acceleration of the degradation kinetics of ITZ relative to paste occurs due to the large increase in porosity generated by the dissolution of portlandite. However, the relative difference remains small. In contrast, the more pronounced chemical degradation of ITZ results in a much greater decrease in the mechanical properties of the paste / aggregate bond compared to paste.

5. Bibliography

- Adenot, F., 1992. Durabilité du béton : Caractérisation et modélisation des processus physiques et chimiques de dégradation du béton. Université d'Orléans.
- Adenot, F., Buil, M., 1992. Modelling of the corrosion of the cement paste by deionized water. Bull. Seismol. Soc. Am. 83, 5–6.
- Adenot, F., Faucon, P., 1996. Modélisation du comportement à long terme des bétons utilisés dans le stockage des déchets radioactifs, in: International RILEM Conference on Concrete: From Material to Structure. pp. 277–288.
- Alhussainy, F., Hasan, H.A., Rogic, S., Neaz Sheikh, M., Hadi, M.N.S., 2016. Direct tensile testing of Self-Compacting Concrete. Constr. Build. Mater. 112, 903–906. https://doi.org/10.1016/j.conbuildmat.2016.02.215
- Bažant, Z.P., Cedolin, L., 1993. Why direct tension test specimens break flexing to the side. J. Struct. Eng. 119, 1101–1113.
- Burlion, N., Rougelot, T., Bernard, D., Skoczylas, F., 2007. Apport de la microtomographie pour l'étude de la fissuration des matériaux cimentaires sous lixiviation 23–25.
- Camps, G., 2008. Etude des interactions chemo-mécaniques pour la simulation du cycle de vie d'un élément de stockage en béton. Université de Toulouse, Université Toulouse III-Paul Sabatier.
- Carde, C., 1996. Caractérisation et modélisation de l'altération des propriétés mécaniques due à la lixiviation des matériaux cimentaires. Toulouse, INSA.
- Carde, C., François, R., 1997a. Effect of the leaching of calcium hydroxide from cement paste on mechanical and physical properties. Cem. Concr. Res. 27, 539–550. https://doi.org/10.1016/S0008-8846(97)00042-2
- Carde, C., François, R., 1997b. Effect of ITZ leaching on durability of cement-based materials. Cem. Concr. Res. 27, 971–978.
- Carde, C., François, R., Torrenti, J.M., 1996. Leaching of both calcium hydroxide and C-S-H from cement paste: Modeling the mechanical behavior. Cem. Concr. Res. 26, 1257–1268. https://doi.org/10.1016/0008-8846(96)00095-6
- Dong, W., Wu, Z., Zhou, X., 2016. Fracture Mechanisms of Rock-Concrete Interface: Experimental and Numerical. J. Eng. Mech. 142, 04016040. https://doi.org/10.1061/(asce)em.1943-7889.0001099
- Ferro, G., 1994. Effetti di scala sulla resistenza a trazione dei materiali. Politecnico di Torino.
- Gerard, B., Pijaudier-Cabot, G., Laborderie, C., 1998. Coupled diffusion-damage modelling and the implications on failure due to strain localisation. Int. J. Solids Struct. 35, 4107–4120. https://doi.org/10.1016/S0020-7683(97)00304-1
- Heukamp, F., Ulm, F.-J., Germaine, J., 2002. Mechanical properties of calcium-leached cement pastes. Cem. Concr. Res. 31, 767–774. https://doi.org/10.1016/s0008-8846(01)00472-0
- Heukamp, F.H., 2003. Chemomechanics of calcium leaching of cement-based materials at different scales: The role of CH-dissolution and CSH degradation on strength and durability performance of materials and structures. Massachusetts Institute of Technology.
- Heukamp, F.H., Ulm, F.J., Germaine, J.T., 2003. Poroplastic properties of calcium-leached cement-based materials. Cem. Concr. Res. 33, 1155–1173. https://doi.org/10.1016/S0008-

- 8846(03)00024-3
- Hild, F., 2004. Mesure de champs de déplacement par corrélation d'images et applications en mécanique des solides.
- Jebli, M., 2016. Caractérisation à l'échelle locale des propriétés mécaniques de l'interphase pâte de ciment-granulat et application à la lixiviation. Université de Montpellier.
- Jebli, M., Jamin, F., Pelissou, C., Malachanne, E., Garcia-Diaz, E., El Youssoufi, M.S., 2018. Leaching effect on mechanical properties of cement-aggregate interface. Cem. Concr. Compos. 87, 10–19. https://doi.org/10.1016/j.cemconcomp.2017.11.018
- Kamali, S., Gérard, B., Moranville, M., 2003. Modelling the leaching kinetics of cement-based materials Influence of materials and environment. Cem. Concr. Compos. 25, 451–458. https://doi.org/10.1016/S0958-9465(02)00085-9
- Le Bellégo, C., 2001. Couplage chimie mécanique dans les structures en béton armé attaquées par l'eau--Etude expérimentale et analyse numérique. Ec. Norm. Supérieure Cachan.
- Le Bellégo, C., Gérard, B., Pijaudier-Cabot, G., 2000. Chemo-mechanical effects in mortar beams subjected to water hydrolysis. J. Eng. Mech. 126, 266–272.
- Lea, F.M., 2012. The action of ammonium salts on concrete. Mag. Concr. Res. 17, 115–116. https://doi.org/10.1680/macr.1965.17.52.115
- Lhonneur, J., Girboveanu, A., Jamin, F., Pélissou, C., Monerie, Y., El Youssoufi, M.S., 2019. Étude statistique de la réponse mécanique lors d'essais de traction directe à l'échelle locale, in: 14e Colloque National En Calcul de Structures-CSMA 2019.
- Mainguy, M., Tognazzi, C., Torrenti, J.M., Adenot, F., 2000. Modelling of leaching in pure cement paste and mortar. Cem. Concr. Res. 30, 83–90. https://doi.org/10.1016/S0008-8846(99)00208-2
- Mier, J.G.M. Van, Vliet, M.R.A. Van, 2002. Uniaxial tension test for the determination of fracture parameters of concrete: state of the art. Eng. Fract. Mech. 69, 235–247.
- Monteiro, J.J.M., Mehta, P.K., 1985. Ettringite formation on the aggregate—cement paste interface. Cem. Concr. Res. 15, 378–380.
- Nguyen, V., 2005. Couplage dégradation chimique comportement en compression du béton. Ecole Nationale des Ponts et Chaussées.
- Öztekin, E., Pul, S., Hüsem, M., 2016. Experimental determination of Drucker-Prager yield criterion parameters for normal and high strength concretes under triaxial compression. Constr. Build. Mater. 112, 725–732. https://doi.org/10.1016/j.conbuildmat.2016.02.127
- Petersson, P.-E., 1981. Crack growth and development of fracture zones in plain concrete and similar materials.
- Revertegat, E., Richet, C., Gégout, P., 1992. Effect of pH on the durability of cement pastes. Cem. Concr. Res. 22, 259–272. https://doi.org/10.1016/0008-8846(92)90064-3
- Rougelot, T., Burlion, N., Bernard, D., Skoczylas, F., 2010. About microcracking due to leaching in cementitious composites: X-ray microtomography description and numerical approach. Cem. Concr. Res. 40, 271–283. https://doi.org/10.1016/j.cemconres.2009.09.021
- Saito, H., Nakane, S., Ikari, S., Fujiwara, A., 1992. Preliminary experimental study on the deterioration of cementitious materials by an acceleration method. Nucl. Eng. Des. 138, 151–

- 155. https://doi.org/10.1016/0029-5493(92)90290-C
- Swaddiwudhipong, S., Lu, H.R., Wee, T.H., 2003. Direct tension test and tensile strain capacity of concrete at early age. Cem. Concr. Res. 33, 2077–2084. https://doi.org/10.1016/S0008-8846(03)00231-X
- Wattrisse, B., Chrysochoos, A., Muracciole, J.-M., Némoz-Gaillard, M., 2001. Analysis of strain localization during tensile tests by digital image correlation. Exp. Mech. 41, 29–39.
- Zhou, F.P., 1988. Some aspects of tensile fracture behaviour and structural response of cementitious materials.